Journal of Sound and Vibration (2002) **256**(1), 103–129
doi:10.1006/jsvi.2001.4202, available online at http://www.idealibrary.com on IDEAL®

FREE VIBRATIONS OF MULTILAYERED PLATES BASED ON A MIXED VARIATIONAL APPROACH IN CONJUNCTION WITH GLOBAL PIECEWISE-SMOOTH FUNCTIONS

A. Messina

Dipartimento di Ingegneria dell'Innovazione, Università di Lecce, Via Monteroni, 73100 *Lecce, Italy*.
E-mail: *arcangelo.messina@unile.it*

(*Received* 24 *April* 2001, *and in final form* 15 *January* 2002)

This paper presents a two-dimensional model for the analysis of freely vibrating laminated plates. The governing differential equations, associated boundary conditions and constitutive equations are derived from Reissner's mixed variational theorem. Both the governing differential equations and the related boundary conditions are presented in terms of resultant stresses and displacements. The model is able to provide the results for the corresponding three-dimensional theory. Such a performance is guaranteed from an appropriate expansion of relevant kinetic and stress quantities through the thickness of the multilayered plate. The expansion is realized by using a novel selection of global piecewise-smooth functions (GPSFs). The number of GPSFs can be arbitrarily increased to achieve a two-dimensional plate theory which is, at least, as accurate as that of a full layerwise theory. It is also shown that GPSFs permit to deal a multilayered plate as if it was virtually made of a single layer. Indeed, the theory need not explicitly introduce continuity conditions for both displacements and relevant stresses. The performance of the present two-dimensional model in conjunction with the global piecewise-smooth functions is tested and discussed by comparing its resulting *eigen-parameters*, for a class of simply supported plates, with those of other two-dimensional models and with those existing of the exact three-dimensional theory.

1. INTRODUCTION

The theories describing the dynamic behaviour of a laminated plate during its free vibrations can be divided into four main categories which, in the order of complexity involved in the models, can be defined as the (i) classical plates theory (CPT), (ii) first order shear deformable theory (FSDT), (iii) higher order shear deformable theories (HSDT) and (iv) three-dimensional theories (3-D). The acronyms used for the two-dimensional theories are used in this paper for those models which describe in a global sense (through the whole thickness of the laminate) the related assumptions in the frame of the *method of the hypotheses*. In this respect, references [1–3] can be considered as the leading FSDT models for static and dynamic studies while references [4, 5] are monographs dedicated to the applications of both CPT and FSDT. As far as HSDT models are concerned, references [6–12] are of particular relevance.

With respect to the three-dimensional model, which has rarely been solved in exact form in engineering vibration problems, all the previous two-dimensional models have inherent limitations although they constitute a useful engineering alternative in several practical

0022-460X/02/$35.00

applications. Recent developments have, however, also indicated that two-dimensional models need to be further refined. In particular, for fibre-reinforced laminates the thickness of the laminated plates together with the variety of the materials employed have a remarkable influence on the related dynamical behaviour of composite multilayered plates. In this regard, therefore, more sophisticated two-dimensional theories are expected to give more reliable results.

The main drawbacks of the aforementioned theories (CPT, FSDT, HSDT) are the possible violations concerning the continuity of interlaminar transversal stresses. In this respect, several models exist to account for the continuity requirements at the interfaces of different layers (see, for example, references [13–19]). Such models deal with a distribution of the displacement components and related transversal stresses that come mainly from an extrapolation of CPTs, FSDTs, and PSDPTs to a layer-by-layer level. However, as it has been verified [20–22], such continuity requirements should possibly be integrated with suitable shape functions that might better model displacement and stress quantities besides possibly increasing the number of degrees of freedom [23–25]. In particular, Nosier *et al.* [24] showed how a generalized layerwise theory (LWPT) [23] was able to evaluate frequencies which agreed quite well with those of the three-dimensional theory of elasticity. However, such a layerwise theory was developed without an *a priori* fulfilment of the transverse stress continuity. The continuity requirements were related to the generalized displacement components that were assumed to be linear throughout the layers considered. As far as the laminated plate theory introduced by Soldatos [25] is concerned, it is, similar to reference [23], a displacement-based theory. In such a generalized theory, the continuity requirements, concerning the transverse shear stresses, were consistently imposed by Hamilton's principle in conjunction with Lagrange multipliers. Unfortunately, Soldatos [25] deals with theoretical work that has not yet been supported by numerical comparisons.

In order to avoid the shortcomings of displacement-based theories (after assuming a displacement field the constitutive equations naturally lead to discontinuous transverse stresses) the present work was directed towards a mixed-variational approach, where a plausible assumption is made for both displacement and stresses.

This work deals with a two-dimensional theory tailored for dynamical studies of freely vibrating laminated plates. The theory is mainly based upon Reissner's works [26, 27]. However, it is stressed that this work does not constitute the first attempt to build a two-dimensional model based on this choice. Indeed, Murakami [28] and Toledano and Murakami [29] were the first to develop an analytical model for studying laminated composite plates in the frame of static studies of laminated plates. In both papers a linear assumption of the in-plane displacement components was made through the layers of the laminate and the shear transverse stresses were modelled by using a quadratic variation. More recently, Carrera [30–32] extended the application of Reissner's variational theorem to corresponding dynamic studies of vibrations of multilayered plates and shells as well as accounting for the effects of the normal stresses.

As far as the interests of this work are concerned, reference [32] deserves particular attention. Carrera [32] compares several two-dimensional models from which a layerwise model (LW4) is found to be the most accurate model to describe the dynamic behaviour of laminated plates. Such a layerwise model was introduced by using Legendre polynomials to describe displacements and stresses through the thickness of each layer of the laminate. In addition to this, after getting the equilibrium and compatibility equations with the related boundary conditions for each layer, a further step explicitly imposed the continuity requirements to derive the governing equations and boundary conditions for the whole laminate. The theory resulted in a layerwise model having an increasing complexity depending on the number of layers.

In addition to the previous studies, based on Reissner's works [26, 27], Messina [22] investigated the possibility to arbitrarily expand the number of degrees of freedom in a global sense through the thickness of the laminate by using certain orthogonal polynomials that properly satisfied the relevant boundary conditions. This procedure provided an expansion, which is independent of the number of layers and the theory did not require an additional *a posteriori* mathematical treatment to explicitly impose the interlaminar continuity requirements and the external boundary conditions. The models presented in reference [22] were, however, characterized by the following limitations: (i) the approximating functions for transverse shear stress and in-plane displacements were continuous with its first derivatives; (ii) normal effects were neglected ($W(x, y, z; t) = w(x, y; t)$; $\sigma_z = 0$).

Based on the encouraging results that were obtained for the mixed model (M2D) in reference [22], in the present work both assumptions (i, ii) are removed completely thereby retaining the advantages presented in reference [22]. Namely, the present model constitutes an extension to take into account an arbitrarily high number of degrees of freedom with an attempt to account for the relevant three-dimensional behaviours by using a two-dimensional model. It is believed that this objective can be obtained by fulfilling all the requirements of the exact theory (satisfying all continuity requirements in a strict sense rather than in a weak form [22] and satisfying the related boundary conditions). For this reason, the classical expansion in series has been generalized from continuously smooth functional bases to bases characterized by global piecewise-smooth functions (GPSFs).

It is hereafter shown that such functions make the development of a mixed-based laminated plate theory that avoids the explicit introduction of continuity requirements for both stress and displacement components possible. The continuity requirements are inherently obtained by superimposing GPSFs.

Such GPSFs are obtained from a novel, although not unique selection, in a set of dependent functions symbolically belonging to a graph. The graph is made by an arrangement of delayed, scaled and turned over known continuous smooth functions, that satisfy relevant requested boundary conditions in the problem being dealt with. Relevant questions of non-uniqueness and independence are discussed, proved and numerically tested in the frame of a *best approximation in the mean* to a prescribed function [33].

Finally, as far as the mathematical two-dimensional model is concerned, once the governing differential equations of motion and the related boundary conditions are consistently obtained for general material arrangements (angle and cross-ply lay-ups, symmetrically stacked or not), they are presented as depending on displacements and generalized stresses. The performances of such a two-dimensional model in conjunction with the GPSFs have been tested by comparing the eigenfrequencies of the present model to those frequencies of certain simply supported plates; that is, the exact three-dimensional eigenfrequencies which are known [24]. Further comparisons with respect to existing two-dimensional layerwise theories [24, 32] also provide support for the excellent behaviour of the present model.

2. THE GENERALIZED TWO-DIMENSIONAL MIXED-BASED PLATE MODEL (M3D)

Consider a rectangular plate having a constant thickness h, an axial length L_x, and a transversal length L_y, (Figure 1). The in-plane and normal co-ordinate length parameters are denoted with x, y and z, respectively, where U, V and W represent the corresponding

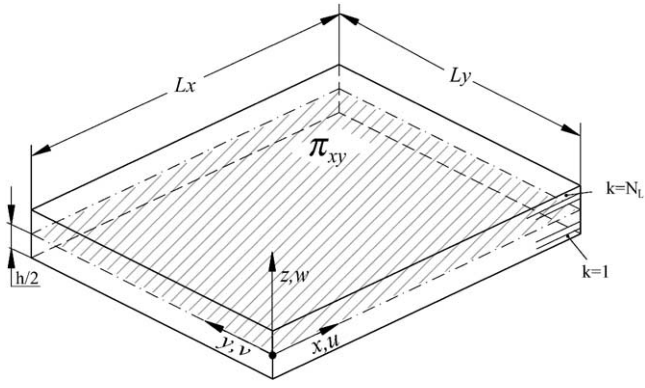

Figure 1. Nomenclature and co-ordinate system of the laminated plate.

displacement components. The plate is made of an arbitrary number, N_L, of linearly elastic monoclinic layers (Figure 1).

The present general laminated plate theory begins with the following displacement and stress expansions:

$$U(x, y, z; t) = \Phi(z)_{1j}\, u(x, y; t)_j, \qquad V(x, y, z; t) = \Phi(z)_{2j}\, v(x, y; t)_j,$$

$$W(x, y, z; t) = \Phi(z)_{3j}\, w(x, y; t)_j. \tag{1}$$

$$\tau(x, y, z; t)_{yz} = \alpha(z)_p\, \tau(x, y; t)_{yzp}, \qquad \tau(x, y, z; t)_{xz} = \beta(z)_p\, \tau(x, y; t)_{xzp},$$

$$\sigma(x, y, z; t)_z = \eta(z)_p\, \sigma(x, y; t)_{zp}. \tag{2}$$

where in each single equation, (1, 2), the indices (j, $p = 1, \ldots, N_u, N_\sigma$) are assumed to be repeated in place of the relevant summation. This convention is later considered unless differently specified. Moreover, without loss of generality, the approximating functions ($\Phi(z)_{1j}$, $\Phi(z)_{2j}$, $\Phi(z)_{3j}$, $\alpha(z)_p$, $\beta(z)_p$, $\eta(z)_p$) expressed through the z-co-ordinate are considered dimensionless and the functions defined in the middle plane (π_{xy}, in Figure 1) have the corresponding dimensions of displacement and stress.

If such functions [$\Phi(z)_{1j}$, $\Phi(z)_{2j}$, $\Phi(z)_{3j}$, $\alpha(z)_p$, $\beta(z)_p$, $\eta(z)_p$] defined through the z-co-ordinate are considered to be known, equations (1, 2) should permit the development of the present theory using degrees of freedom that are defined in the middle plane of the plate. Such functions are thought as globally defined through the whole thickness of the laminate, i.e., $-\frac{1}{2} \leqslant z/h = \xi \leqslant \frac{1}{2}$, rather than at each layer level. Moreover, they are chosen in order to satisfy the boundary conditions on the top and bottom of the plate. In particular, as far as the transverse stress components (τ_{yz}, τ_{xz}, σ_z) are concerned, the relevant approximating functions ($\alpha(z)_p$, $\beta(z)_p$, $\eta(z)_p$) should assume zero values at the bottom and top of the laminate. This choice will dictate at any expansion level (N fixed) the zero-traction boundary conditions on the lateral surfaces of the laminated plate. The case for the displacement components is different; the expanding functions ($\Phi(z)_{1j}$, $\Phi(z)_{2j}$, $\Phi(z)_{3j}$) should not introduce any constraint on the displacement field and, therefore, a complete unconstrained base should be used. Both mathematical aspects will be discussed further in section 3.

Based on the assumed displacement field the kinetic equations can be obtained through the three-dimensional elasticity as follows [$(\,)' = (\mathrm{d}/\mathrm{d}z)(\,)$; $(\,)_{,x} = \partial(\,)/\partial x$; to carry out layer by layer]:

$$\varepsilon_x = \Phi_{1j} u_{j,x}, \quad \varepsilon_y = \Phi_{2j} v_{j,y}, \quad \varepsilon_z = \Phi'_{3j} w_j,$$

$$\gamma_{xy} = \Phi_{1j} u_{j,y} + \Phi_{2j} v_{j,x}, \quad \gamma_{xz} = \Phi'_{1j} u_j + \Phi_{3j} w_{j,x}, \quad \gamma_{yz} = \Phi'_{2j} v_j + \Phi_{3j} w_{j,y}. \tag{3}$$

In accordance with the adopted mixed-based approach [22, 27, 30–32], generalized Hooke's law, referred to the kth layer, can be considered in the following form:

$$\left\langle \begin{pmatrix} \sigma_x^k \\ \sigma_y^k \\ \tau_{xy}^k \end{pmatrix} \right\rangle = \begin{bmatrix} \begin{bmatrix} C_{11}^k & C_{12}^k & C_{16}^k \\ C_{12}^k & C_{22}^k & C_{26}^k \\ C_{16}^k & C_{26}^k & C_{66}^k \end{bmatrix} & \begin{bmatrix} 0 & 0 & C_{13}^k \\ 0 & 0 & C_{23}^k \\ 0 & 0 & C_{36}^k \end{bmatrix} \\ \begin{bmatrix} 0 & 0 & 0 \\ 0 & 0 & 0 \\ C_{13}^k & C_{23}^k & C_{36}^k \end{bmatrix} & \begin{bmatrix} C_{44}^k & C_{45}^k & 0 \\ C_{45}^k & C_{55}^k & 0 \\ 0 & 0 & C_{33}^k \end{bmatrix} \end{bmatrix} \cdot \left\langle \begin{pmatrix} \varepsilon_x^k \\ \varepsilon_y^k \\ \gamma_{xy}^k \end{pmatrix} \right\rangle = \begin{bmatrix} \mathbf{C}_{126}^k & \mathbf{D}^k \\ \mathbf{D}^{k\mathrm{T}} & \mathbf{C}_{345}^k \end{bmatrix} \begin{pmatrix} \mathbf{e}_{in} \\ \mathbf{e}_{ou} \end{pmatrix}$$

$$\left\langle \begin{pmatrix} \tau_{yz}^k \\ \tau_{xz}^k \\ \sigma_z^k \end{pmatrix} \right\rangle \qquad \left\langle \begin{pmatrix} \gamma_{yz}^k \\ \gamma_{xz}^k \\ \varepsilon_z^k \end{pmatrix} \right\rangle \tag{4}$$

from which, based on the circumstances of the adopted approach [22, 27, 30–32], equation (4) can be re-arranged as follows:

$$\sigma_{in} = (\mathbf{C}_{126}^k - \mathbf{D}^k (\mathbf{C}_{345}^k)^{-1} \mathbf{D}^{k\mathrm{T}}) \mathbf{e}_{in} + \mathbf{D}^k (\mathbf{C}_{345}^k)^{-1} \sigma_{ou},$$

$$\mathbf{e}_{ou} = (\mathbf{C}_{345}^k)^{-1} \sigma_{ou} - (\mathbf{C}_{345}^k)^{-1} \mathbf{D}^{k\mathrm{T}} \mathbf{e}_{in}. \tag{5}$$

The mixed variational equations [22, 27, 30–32] can be then considered for the dynamic case of freely vibrating systems in the following equation:

$$\int_{Vol} \sigma_{in}^{\mathrm{T}} \delta \mathbf{e}_{in}^{(\mathrm{G})} + \sigma_{ou}^{\mathrm{T}} \delta \mathbf{e}_{ou}^{(\mathrm{G})} + \delta \sigma_{ou}^{\mathrm{T}} (\mathbf{e}_{ou}^{(\mathrm{G})} - \mathbf{e}_{ou}^{(\mathrm{C})}) + \rho (\ddot{U}\, \delta U + \ddot{V} \delta V + \ddot{W}\, \delta W)\, \mathrm{d}\, Vol = 0, \tag{6}$$

where the superscript T stands for the transpose operator. The superscripts in parentheses (G, C) are stating that the relevant out of plane strains ($\mathbf{e}_{ou}$) should be introduced, into equation (6), by using the geometric equations (3) and the constitutive equations (5) respectively. Conversely, the in-plane strains are always related to the displacement by equations (3). Finally, in-plane (σ_{in}) and out-of-plane stresses (σ_{ou}) should be assessed by using the constitutive equations (5) and the assumed field equations (2) respectively.

Therefore, applying equation (6) according to equations (1–5), carrying out the relevant integrations by parts, not reported here for brevity's sake, and finally with a view of considering the z-integrations through the whole thickness of the laminate, the governing differential equations are obtained together with the relevant boundary conditions:

$$\delta u_i: \quad N_{xi,x} + N_{xy1i,y} - Q_{1pi} = \rho_{\mathrm{o}}^{1j,1i} \ddot{u}_j,$$

$$\delta v_i: \quad N_{yi,y} + N_{xy2i,x} - Q_{2pi} = \rho_{\mathrm{o}}^{2j,2i} \ddot{v}_j,$$

$$\delta w_i: \quad V_{xzpi,x} + V_{yzpi,y} - Q_{3pi} = \rho_{\mathrm{o}}^{3j,3i} \ddot{w}_j. \tag{7}$$

Along $x = 0$, L_x:

$$N_{xi} = 0, \text{ or } u_i; \quad N_{xy2i} = 0, \text{ or } v_i; \; V_{xzpi} = 0, \text{ or } w_i.$$

Along $y = 0$, L_y:

$$N_{yi} = 0, \text{ or } v_i; \quad N_{xy1i} = 0, \text{ or } u_i; \; V_{yzpi} = 0, \text{ or } w_i \tag{8}$$

and the consistent constitutive equations:

$$\mathbf{A} \cdot \boldsymbol{\tau} = \mathbf{B}^u \cdot \mathbf{u} + \mathbf{B}^v \cdot \mathbf{v} + \mathbf{B}^w \cdot \mathbf{w}, \tag{9}$$

where the quantities presented in equations (7, 8) corresponds to the following relations:

$$(N_{xi}, N_{yi}) = \int_{-h/2}^{h/2} (\sigma_x, \sigma_y) \cdot (\Phi_{1i}, \Phi_{2i}) \, \mathrm{d}z,$$

$$(N_{xy1i}, N_{xy2i}) = \int_{-h/2}^{h/2} \tau_{xy} \cdot (\Phi_{1i}, \Phi_{2i}) \, \mathrm{d}z, \quad (V_{xzpi}, V_{yzpi}) = \int_{-h/2}^{h/2} \Phi_{3i}(\beta_p, \alpha_p) \, (\tau_{xzp}, \tau_{yzp}) \, \mathrm{d}z,$$

$$(Q_{1pi}, Q_{2pi}, Q_{3pi}) = \int_{-h/2}^{h/2} (\Phi'_{1i}, \Phi'_{2i}, \Phi'_{3i})(\beta_p, \alpha_p, \eta_p) \, (\tau_{xzp}, \tau_{yzp}, \sigma_{zp}) \, \mathrm{d}z, \tag{10}$$

$$\rho_o^{lm,nq} = \int_{-h/2}^{h/2} \rho \Phi_{lm}, \, \Phi_{nq} \, \mathrm{d}z \tag{11}$$

with ρ being the volumetric density of the material. Finally, the matrices reported in equation (9) have the following form:

$$\mathbf{A} = \begin{bmatrix} \mathbf{A_{11}} & \mathbf{A_{12}} & \mathbf{0} \\ \mathbf{A_{12}^T} & \mathbf{A_{22}} & \mathbf{0} \\ \mathbf{0} & \mathbf{0} & \mathbf{A_{33}} \end{bmatrix}, \quad \mathbf{B}^u = \begin{bmatrix} \mathbf{0} & \mathbf{0} & \mathbf{0} \\ \mathbf{B_{21}^u} & \mathbf{0} & \mathbf{0} \\ \mathbf{0} & \mathbf{B_{32}^u} & \mathbf{B_{33}^u} \end{bmatrix}, \quad \mathbf{B}^v = \begin{bmatrix} \mathbf{B_{11}^v} & \mathbf{0} & \mathbf{0} \\ \mathbf{0} & \mathbf{0} & \mathbf{0} \\ \mathbf{0} & \mathbf{B_{32}^v} & \mathbf{B_{33}^v} \end{bmatrix},$$

$$\mathbf{B}^w = \begin{bmatrix} \mathbf{0} & \mathbf{0} & \mathbf{B_{13}^w} \\ \mathbf{0} & \mathbf{B_{22}^w} & \mathbf{0} \\ \mathbf{B_{31}^w} & \mathbf{0} & \mathbf{0} \end{bmatrix}, \tag{12}$$

$$\boldsymbol{\tau} = (\tau_{yz1}, \ldots, \tau_{yzN\sigma}; \; \tau_{xz1} \ldots, \tau_{xzN\sigma}; \; \sigma_{z1} \ldots, \sigma_{zN\sigma})^{\mathrm{T}},$$

$$\mathbf{u} = (u_1, \ldots, u_{Nu}; \; u_{1,x} \ldots, u_{Nu,x}; \; u_{1,y} \ldots, u_{Nu,y})^{\mathrm{T}},$$

$$\mathbf{v} = (v_1, \ldots, v_{Nu}; \; v_{1,x} \ldots, v_{Nu,x}; \; v_{1,y} \ldots, v_{Nu,y})^{\mathrm{T}},$$

$$\mathbf{w} = (w_1, \ldots, w_{Nu}; \; v_{1,x} \ldots, v_{Nu,x}; \; v_{1,y} \ldots, v_{Nu,y})^{\mathrm{T}}, \tag{13}$$

where each submatrix in ($\mathbf{A}$, $\mathbf{B}^u$, $\mathbf{B}^v$, $\mathbf{B}^w$) is constituted by the following components:

$$\mathbf{A_{11}} = \int_{-h/2}^{h/2} E_{11}^k \begin{bmatrix} \alpha_1\alpha_1 & \cdots & \alpha_1\alpha_{N\sigma} \\ \vdots & \ddots & \vdots \\ \alpha_{N\sigma}\alpha_1 & \cdots & \alpha_{N\sigma}\alpha_{N\sigma} \end{bmatrix} \mathrm{d}z, \quad \mathbf{A_{12}} = \int_{-h/2}^{h/2} E_{12}^k \begin{bmatrix} \beta_1\alpha_1 & \cdots & \beta_{N\sigma}\alpha_1 \\ \vdots & \ddots & \vdots \\ \beta_1\alpha_{N\sigma} & \cdots & \beta_{N\sigma}\alpha_{N\sigma} \end{bmatrix} \mathrm{d}z,$$

$$\mathbf{A_{22}} = \int_{-h/2}^{h/2} E_{22}^k \begin{bmatrix} \beta_1\beta_1 & \cdots & \beta_1\beta_{N\sigma} \\ \vdots & \ddots & \vdots \\ \beta_{N\sigma}\beta_1 & \cdots & \beta_{N\sigma}\beta_{N\sigma} \end{bmatrix} \mathrm{d}z, \quad \mathbf{A_{33}} = \int_{-h/2}^{h/2} E_{33}^k \begin{bmatrix} \eta_1\eta_1 & \cdots & \eta_1\eta_{N\sigma} \\ \vdots & \ddots & \vdots \\ \eta_{N\sigma}\eta_1 & \cdots & \eta_{N\sigma}\eta_{N\sigma} \end{bmatrix} \mathrm{d}z. \tag{14}$$

$$\mathbf{B_{21}^u} = \int_{-h/2}^{h/2} \begin{bmatrix} \beta_1\Phi'_{11} & \cdots & \beta_1\Phi'_{1Nu} \\ \vdots & \ddots & \vdots \\ \beta_{N\sigma}\Phi'_{11} & \cdots & \beta_{N\sigma}\Phi'_{1Nu} \end{bmatrix} \mathrm{d}z, \quad \mathbf{B_{32}^u} = \int_{-h/2}^{h/2} F_{31}^k \cdot \begin{bmatrix} \eta_1\Phi_{11} & \cdots & \eta_1\Phi_{1Nu} \\ \vdots & \ddots & \vdots \\ \eta_{N\sigma}\Phi_{11} & \cdots & \eta_{N\sigma}\Phi_{1Nu} \end{bmatrix} \mathrm{d}z,$$

$$\mathbf{B_{33}^u} = \int_{-h/2}^{h/2} F_{33}^k \cdot \begin{bmatrix} \eta_1\Phi_{11} & \cdots & \eta_1\Phi_{1Nu} \\ \vdots & \ddots & \vdots \\ \eta_{N\sigma}\Phi_{11} & \cdots & \eta_{N\sigma}\Phi_{1Nu} \end{bmatrix} \mathrm{d}z. \tag{15}$$

$$\mathbf{B_{11}^v} = \int_{-h/2}^{h/2} \begin{bmatrix} \alpha_1\Phi'_{21} & \cdots & \alpha_1\Phi'_{2Nu} \\ \vdots & \ddots & \vdots \\ \alpha_{N\sigma}\Phi'_{21} & \cdots & \alpha_{N\sigma}\Phi'_{2Nu} \end{bmatrix} \mathrm{d}z, \quad \mathbf{B_{32}^v} = \int_{-h/2}^{h/2} F_{33}^k \cdot \begin{bmatrix} \eta_1\Phi_{21} & \cdots & \eta_1\Phi_{2Nu} \\ \vdots & \ddots & \vdots \\ \eta_{N\sigma}\Phi_{21} & \cdots & \eta_{N\sigma}\Phi_{2Nu} \end{bmatrix} \mathrm{d}z,$$

$$\mathbf{B_{33}^v} = \int_{-h/2}^{h/2} F_{32}^k \cdot \begin{bmatrix} \eta_1\Phi_{21} & \cdots & \eta_1\Phi_{2Nu} \\ \vdots & \ddots & \vdots \\ \eta_{N\sigma}\Phi_{21} & \cdots & \eta_{N\sigma}\Phi_{2Nu} \end{bmatrix} \mathrm{d}z. \tag{16}$$

$$\mathbf{B_{13}^w} = \int_{-h/2}^{h/2} \begin{bmatrix} \alpha_1\Phi_{31} & \cdots & \alpha_1\Phi_{3Nu} \\ \vdots & \ddots & \vdots \\ \alpha_{N\sigma}\Phi_{31} & \cdots & \alpha_{N\sigma}\Phi_{3Nu} \end{bmatrix} \mathrm{d}z, \quad \mathbf{B_{22}^w} = \int_{-h/2}^{h/2} \begin{bmatrix} \beta_1\Phi_{31} & \cdots & \beta_1\Phi_{3Nu} \\ \vdots & \ddots & \vdots \\ \beta_{N\sigma}\Phi_{31} & \cdots & \beta_{N\sigma}\Phi_{3Nu} \end{bmatrix} \mathrm{d}z,$$

$$\mathbf{B_{31}^w} = \int_{-h/2}^{h/2} \begin{bmatrix} \eta_1\Phi'_{31} & \cdots & \eta_1\Phi'_{3Nu} \\ \vdots & \ddots & \vdots \\ \eta_{N\sigma}\Phi'_{31} & \cdots & \eta_{N\sigma}\Phi'_{3Nu} \end{bmatrix} \mathrm{d}z \tag{17}$$

with the compliance coefficients (E_{11}^k, E_{12}^k, E_{22}^k) and the dimensionless coefficients (F_{31}^k, F_{32}^k, F_{33}^k) that correspond to $((\mathbf{C}_{345}^k)_{11}^{-1}$, $(\mathbf{C}_{345}^k)_{12}^{-1}$, $(\mathbf{C}_{345}^k)_{22}^{-1})$ and (C_{13}^k/C_{33}^k, C_{23}^k/C_{33}^k, C_{36}^k/C_{33}^k) respectively.

The governing equations (7–9) should finally be completed by the remaining constitutive equations that correlate the resultant stress corresponding to σ_{in} to the strains by the constitutive equations (5). However, before completing the full set of two-dimensional equations that govern the dynamics of the plate, an attempt to present such a set of equations in another form may be more convenient.

In particular, after inverting matrix **A** in equation (9), the transverse stress could be posed in terms of the displacement components by using the same equation (9) once it is pre-multiplied by matrix **G**:

$$\mathbf{G} = \begin{bmatrix} \mathbf{G_{11}} & \mathbf{G_{12}} & \mathbf{0} \\ \mathbf{G_{12}^T} & \mathbf{G_{22}} & \mathbf{0} \\ \mathbf{0} & \mathbf{0} & \mathbf{G_{33}} \end{bmatrix} = \begin{bmatrix} \mathbf{A_{11}} & \mathbf{A_{12}} & \mathbf{0} \\ \mathbf{A_{12}^T} & \mathbf{A_{22}} & \mathbf{0} \\ \mathbf{0} & \mathbf{0} & \mathbf{A_{33}} \end{bmatrix}^{-1} \tag{18}$$

to obtain

$$\boldsymbol{\tau} = \mathbf{G} \cdot \mathbf{B}^u \cdot \mathbf{u} + \mathbf{G} \cdot \mathbf{B}^v \cdot \mathbf{v} + \mathbf{G} \cdot \mathbf{B}^w \cdot \mathbf{w}. \tag{19}$$

By inserting equation (19) into relevant equations (10), it is possible to rewrite the governing differential equations of motion (7), and the related boundary conditions (8) as given in

$$\delta u_i: \quad N_{xi,x} + N_{xy1i,y} - Q_{1i} = \rho_o^{1j,1i} \ddot{u}_j, \qquad \delta v_i: \quad N_{yi,y} + N_{xy2i,x} - Q_{2i} = \rho_o^{2j,2i} \ddot{v}_j,$$
$$\delta w_i: \quad V_{xzi,x} + V_{yzi,y} - Q_{3i} = \rho_o^{3j,3i} \ddot{w}_j. \tag{20}$$

Along $x = 0, L_x$:

$$N_{xi} = 0, \textit{ or } u_i, \quad N_{xy2i} = 0, \textit{ or } v_i, \; V_{xzi} = 0, \textit{ or } w_i.$$

Along $y = 0, L_y$:

$$N_{yi} = 0, \textit{ or } v_i, \quad N_{xy1i} = 0, \textit{ or } u_i, \; V_{yzi} = 0, \textit{ or } w_i. \tag{21}$$

$Q_{1i}, Q_{2i}, Q_{3i}, V_{xzi}, V_{yzi}$ being correspondent, respectively, to $Q_{1pi}, Q_{2pi}, Q_{3pi}, V_{xzpi}, V_{yzpi}$ as illustrated in equations (7, 8, 10). These latter quantities can be then expressed by combining equations (19, 10) in terms of the displacement and displacement gradients to obtain part of the generalized constitutive equations. The remaining constitutive equations can be obtained by correlating the resultant stresses, corresponding to $\boldsymbol{\sigma}_{in}$, to the strains by equations (5, 19) and the relevant resultant stresses of equation (10). Therefore, the algebraic manipulations mentioned result in the following matrix equation (22) that represents the generalized constitutive equations:

$$\begin{pmatrix} \mathbf{N}_x \\ \mathbf{N}_y \\ \mathbf{N}_{xy1} \\ \mathbf{N}_{xy2} \\ \mathbf{V}_{xz} \\ \mathbf{V}_{yz} \\ \mathbf{Q}_1 \\ \mathbf{Q}_2 \\ \mathbf{Q}_3 \end{pmatrix} = \begin{bmatrix} \bar{\mathbf{C}}_{11} & \bar{\mathbf{C}}_{12} & \bar{\mathbf{C}}_{13} & \bar{\mathbf{C}}_{14} & \mathbf{0} & \mathbf{0} & \mathbf{0} & \mathbf{0} & \bar{\mathbf{C}}_{19} \\ & \bar{\mathbf{C}}_{22} & \bar{\mathbf{C}}_{23} & \bar{\mathbf{C}}_{24} & \mathbf{0} & \mathbf{0} & \mathbf{0} & \mathbf{0} & \bar{\mathbf{C}}_{29} \\ & & \bar{\mathbf{C}}_{33} & \bar{\mathbf{C}}_{34} & \mathbf{0} & \mathbf{0} & \mathbf{0} & \mathbf{0} & \bar{\mathbf{C}}_{39} \\ & & & \bar{\mathbf{C}}_{44} & \mathbf{0} & \mathbf{0} & \mathbf{0} & \mathbf{0} & \bar{\mathbf{C}}_{49} \\ & & & & \bar{\mathbf{C}}_{55} & \bar{\mathbf{C}}_{56} & \bar{\mathbf{C}}_{57} & \bar{\mathbf{C}}_{58} & \mathbf{0} \\ & \textit{sym} & & & & \bar{\mathbf{C}}_{66} & \bar{\mathbf{C}}_{67} & \bar{\mathbf{C}}_{68} & \mathbf{0} \\ & & & & & & \bar{\mathbf{C}}_{77} & \bar{\mathbf{C}}_{78} & \mathbf{0} \\ & & & & & & & \bar{\mathbf{C}}_{88} & \mathbf{0} \\ & & & & & & & & \bar{\mathbf{C}}_{99} \end{bmatrix} \cdot \begin{pmatrix} \mathbf{u}_{,x} \\ \mathbf{v}_{,y} \\ \mathbf{u}_{,y} \\ \mathbf{v}_{,x} \\ \mathbf{w}_{,x} \\ \mathbf{w}_{,y} \\ \mathbf{u} \\ \mathbf{v} \\ \mathbf{w} \end{pmatrix}. \tag{22}$$

The elements of the coefficients in matrices $\bar{\mathbf{C}}_{ij}$, are given in Appendix A. The vector on the right-hand side is based on relations (13) and the vector on the left-hand side is an assembled vector of ordered corresponding resultant stresses (10). Finally, it should be

noted that in the previous statements N_u and N_σ have been considered to be different but later any consideration of N_u and N_σ will be referred to as $N = N_u = N_\sigma$.

3. THE GLOBAL PIECEWISE-SMOOTH FUNCTIONS (GPSFs)

In section 2 a theory has been developed without mentioning the approximating functions that, once introduced *a posteriori* into the model, can properly configure the displacement and transverse stress components through the whole thickness of the laminate.

Messina [22] used a similar approach in conjunction with a certain family of orthogonal functions. In part the bases used in reference [22] have been extensively used in vibrational studies of rectangular plates (see, for example, references [21, 34–38]). However, such orthogonal functions satisfied the continuity requirements at the interfaces in a weak form. Indeed, the orthogonal functions used in reference [22] were continuous with continuous derivatives and thus any relevant linear combination still preserved such a smoothness. In this paper, besides the introduction of the normal effects in both displacement and stress (section 2), particular functions are introduced in order to overcome the deficiency of smoothness. In both stresses and displacements, the approximating functions should not be continuously smooth but should contain discontinuities similar to those present in the functions that have to be approximated.

In this respect, the idea that leads to the introduction of these functions is 3-fold: (i) it should be accepted that the approximation of a *discontinuous* function by using *discontinuous* functions is probably an easier task than using continuous functions; (ii) if a *singularity* is considered as an additional degree of freedom in the approximating functions, rather than undesired, then a base made up of discontinuous functions should also be able to approximate naturally continuous functions by simply eliminating the contribution of that degree of freedom (*singularity*) in the approximating process; (iii) a *global* linear combination of approximating functions in a whole domain is simpler than a *local* linear combination domain by domain (layer by layer in a plate) because the latter would require additional continuity conditions at the boundaries. For all these points, a base made up of global discontinuous functions, whenever available, should be considered more general than a base constituted of continuously smooth functions such as, for example, Legendre polynomials, Fourier series, etc. These latter bases (as is well known) have inherent difficulties to model discontinuities [39].

In the problem, which being dealt with, the functions one would like to approximate (displacements and transversal stresses through the thickness of the laminate) are C^0-continuous [12, 19]. Therefore, the development of suitable approximating functions (in the latter termed as global piecewise-smooth functions or GPSFs) should be modelled in this respect. Those functions that will be used *a posteriori* in the theory of section 2 are introduced here independently from their particular application in the present theory because it is believed they might be conveniently used in several contexts. In particular, the mathematical performance of such approximating functions is independently discussed in the following frame of the *best approximation in the mean* to a C^0-continuous prescribed function ($f(z)$).

3.1. GPSFs: INDEPENDENCE, UNIQUENESS AND NUMERICAL TESTS

In this section, the possibility to approximate a generic C^0-continuous $f(z)$ (see, for example, Figure 2) in the mean by using GPSFs is investigated. Without losing any

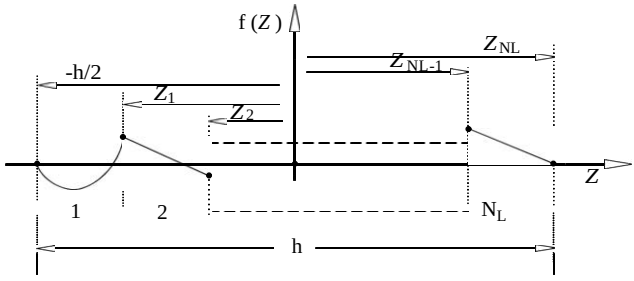

Figure 2. Nomenclature for a C^0-continuous function.

generality the global domain is assumed to be dimensionless in $[-1/2, 1/2]$ with its related independent variable ξ.

In such a context, it is noted here that the best approximation in the mean to a prescribed $f(\xi)$ with respect to linear combinations of known approximating functions $(f(\xi)_1, f(\xi)_2, \ldots, f(\xi)_N)$ is

$$f(\xi)_a = c_1 f(\xi)_1 + c_2 f(\xi)_2 + \cdots + c_N f(\xi)_N, \quad \text{where} \quad \xi \in [-1/2, 1/2] \tag{23}$$

and it consists of determining the coefficients of the linear combination $(c_1, c_2, \ldots, c_N)$ so that the following integral

$$\int_{-1/2}^{1/2} (f(\xi) - c_1 f(\xi)_1 - c_2 f(\xi)_2 - \cdots - c_N f(\xi)_N)^2 \, \mathrm{d}\xi \tag{24}$$

assumes its minimum value. The function $f(\xi)_a$ constitutes the approximation of $f(\xi)$, and it can be evaluated once a set of N linearly independent approximating functions $(f(\xi)_1, f(\xi)_2, \ldots, f(\xi)_N)$ has been chosen. The evaluation can be carried out by equating to zero the first partial derivatives of equation (24) with respect to the coefficients $(c_1, c_2, \ldots, c_N)$. Thus, the approximating process results in solving a system of linear algebraic equations [33]. The linear algebraic system certainly admits a solution since the assumed linear independence of the approximating functions makes the related Gram's determinant [33] non-singular. This problem can be simplified if the approximating functions involved are orthogonal; however, this condition has not been considered here because the approximating functions, considered in the following context, are not globally orthogonal (although such approximating functions will be obtained by joining functions which are originally orthogonal).

In order to rationally obtain a class of GPSFs a particular process of the *best approximation in the mean* of an hypothetical function $f(\xi)$ is considered. For example, the function is constrained in fulfilling the following boundary conditions:

$$f(-1/2) = f(1/2) = 0, \tag{25}$$

besides being C^0-continuous with its derivatives that are discontinuous on the boundary of each single sub-domain (Figure 2). In particular, consider for simplicity that $f(\xi)$ is characterized by two internal points in $[-1/2, 1/2]$ where the derivatives are discontinuous or, equivalently, by three sub-domains that, contained in $[-1/2, 1/2]$, localize the smooth parts of $f(\xi)$.

On the basis of these assumptions it comes quite natural to approximate $f(\xi)$ in the mean in each single sub-domain by using local functional bases such as that reported in

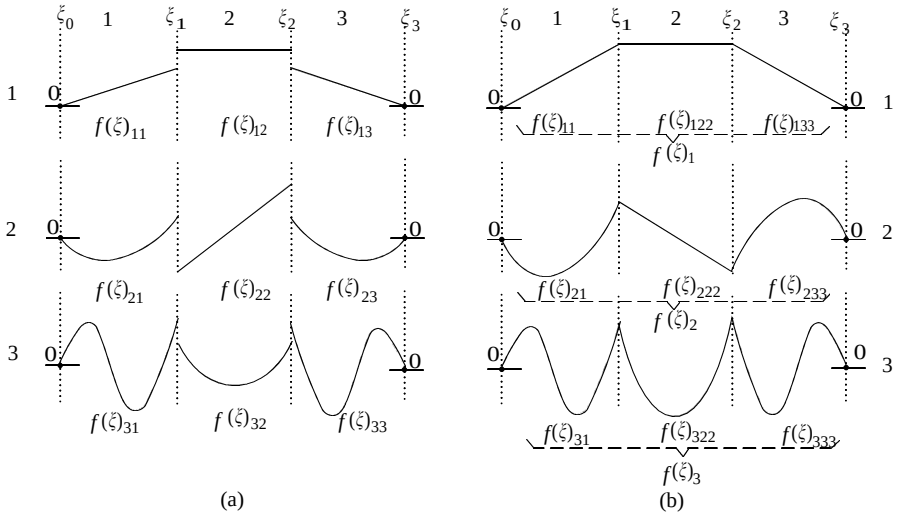

Figure 3. Local (a) and global approximating functions GPSFs (b).

Figure 3(a). In more details, Figure 3(a) shows in each single column (or sub-domain) a complete base up to the first three functional components (row by row). The extreme functions in any row fulfil the related boundary conditions (25) at the boundaries ($\xi_0 = -1/2$ and $\xi_3 = 1/2$) while the base in the middle is not constrained to fulfil any condition apart from the continuity at the internal boundaries (ξ_1, ξ_2). The bases of Figure 3(a) correspond to the functions used in reference [21] and are indicated here in analogy to a consolidated nomenclature that recalls essential beam-type boundary conditions (SF, FF, FS) in the first, second and third sub-domains respectively. The following expressions (26) give an explicit expression for the first three local functional components in a dimensionless domain [0, 1]:

SF-base	*FF-base*
$\sqrt{3}\xi$	1
$4\sqrt{5}(\xi^2 - (3/4)\,\xi)$	$\sqrt{3}(2\xi - 1)$
$\sqrt{7}(15\xi^3 - 20\xi^2 + 6\xi)$	$\sqrt{5}(6\xi^2 - 6\xi + 1)$.

(26)

Equations (26) can be adapted in the relevant sub-domains of Figure 3(a) by simply carrying out a change of variables. Namely, the functional components in the first and third sub-domains of Figure 3(a) (termed SF- and FS-base respectively), were obtained by substituting ξ into SF-base of equation (26) with $(\xi - \xi_0)/(\xi_1 - \xi_0)$ and $(\xi_3 - \xi)/(\xi_3 - \xi_2)$ respectively. The functional components in the second domain of Figure 3(a) were obtained by substituting ξ into FF-base with the quantity $(\xi - \xi_1)/(\xi_2 - \xi_1)$. Evidently, whenever related boundary conditions such as equations (26) are not required, the FF-bases should be used in the place of SF- and FS-base.

Even though these local approximating functions (SF, FF, FS) are able to approximate in the mean to $f(\xi)$ whilst simultaneously fulfilling the boundary conditions (25) (for the

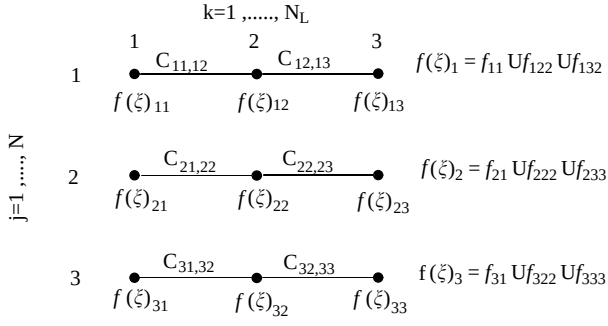

Figure 4. A representative graph for getting GPSFs (Figure 3(b)).

presence of SF- and FS-base), they would also require the explicit introduction of the related continuity conditions at the internal boundaries. Such an explicit introduction might be further complicated whenever the approximation in the mean is not the only problem one is dealing with (as is the case in the present laminated plate theory).

In order to avoid such an explicit introduction of the continuity conditions at the internal boundaries, a question could be raised: whether a global linear combination of C^0-continuous functions is able to realize an approximation in the mean as much as it could be done locally by the standard functional bases (Figure 3(a)). In addition, it might be interesting to investigate if such global C^0-continuous approximating functions can be simply obtained from an *a priori* junction of the previous local functions leading Figure 3(a) to transform into Figure 3(b). That is, Figure 3(b) should be considered to be obtained directly from Figure 3(a) by scaling each single function in its related sub-domain by a coefficient that makes the three global functions reported in Figure 3(b) ($f(\xi)_1$, $f(\xi)_2$, $f(\xi)_3$) globally continuous. The following equation (27) clarifies the concept with respect, for example, to the first global function of Figure 3(b):

$$f(\xi)_1 = \begin{cases} f(\xi)_{11}, & \xi \in (\xi_0,\ \xi_1), \\ f(\xi)_{122} = \dfrac{f(\xi_1)_{11}}{f(\xi_1)_{12}}\, f(\xi)_{12} = C_{11,12}\, f(\xi)_{12}, & \xi \in (\xi_1,\ \xi_2), \\ f(\xi)_{133} = \dfrac{f(\xi_2)_{12}}{f(\xi_2)_{13}}\, \dfrac{f(\xi_1)_{11}}{f(\xi_1)_{12}}\, f(\xi)_{13} = C_{12,13} \cdot C_{11,12} \cdot f(\xi)_{13}, & \xi \in (\xi_2,\ \xi_3). \end{cases} \quad (27)$$

The simple arrangement in equation (27) constitutes a global piecewise-smooth function (GPSF: $f(\xi)_1$). The remaining two GPSFs represented in Figure 3(b), ($f(\xi)_2, f(\xi)_3$) can be similarly obtained by recursively scaling† the local smooth functions in Figure 3(a) as has been shown in equation (27).

The arrangement reported in Figure 3(b) can also be synthesized by the graph in Figure 4 where each single GPSF is represented by a path and each path is made up of nodes and branches. Each node represents a local approximating function and each branch represents a junction characterized by a scaling coefficient ($C_{ij,lm}$). The coefficients represent *a priori* continuity conditions that realize each single GPSF by equation (27). Once it is clear what a graph represents then its nomenclature can be further simplified, thus eliminating the relevant coefficients in all paths.

† Such a recursive scaling process is intended to be carried out always from left (ξ_0) to right (ξ_{N_L}).

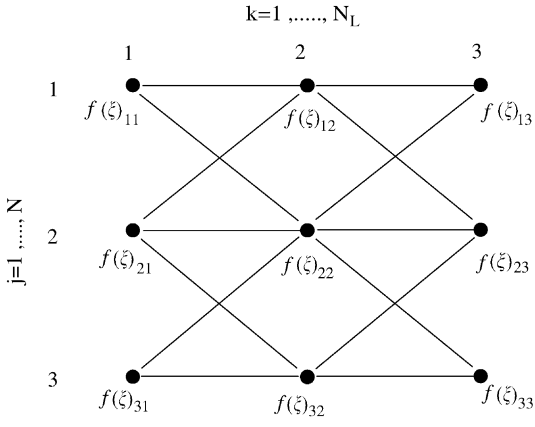

Figure 5. Representation of all extractable paths (GPSFs) from a graph.

After introducing a GPSF, it should be stressed that Figure 4 does not report a complete base of GPSFs. The sense of this statement is related to the evident inability of the three GPSFs of Figure 4 to be effective in an approximation in the mean to a $f(\xi)$ as much as a local approximation (Figure 3(a)) would be able to do domain by domain. Such an inherent inability of the GPSFs reported in Figure 3(b) (or Figure 4) can be explained in different ways. The simplest way is based on an exercise. For example, if $f(\xi)$ corresponds to the following expression:

$$f(\xi) = \begin{cases} 0, & \xi \in (-1/2, \ -1/6), \\ \xi^2 - 1/36, & \xi \in (-1/6, \ +1/6), \\ 0, & \xi \in (+1/6, \ +1/2), \end{cases} \tag{28}$$

it should be evident that a local approximation in the mean by equations (23, 24) to $f(\xi)$ (adapted in the relevant local domains) can be carried out exactly by using the functional components (26) arranged as reported in Figure 3(a). The situation would not be the same whenever the approximation in the mean by equations (23, 24) to $f(\xi)$ is globally carried out by the functional components reported in Figure 3(b) (GPSFs). In this case, it would result in a poor approximation of $f(\xi)$ (28). Such a situation is not acceptable because from a suitable set of GPSFs constituted by polynomial components of Figure 3(a), an exact representation in the mean to a piecewise-smooth polynomial $f(\xi)$, having its maximum degree with a parabola (28), should be expected.

The incompleteness of the GPSFs of Figure 3(b) can be further supported by the fact that a row-by-row selection of N GPSFs (Figure 4) is arbitrary. Indeed, any other arbitrary choice different from a row-by-row selection could be a suitable set of GPSFs for approximating in the mean to a prescribed function $f(\xi)$. In this regard, Figure 5 makes it clear that N^{N_L} GPSFs might be extracted from a graph. Therefore, the N GPSFs row-by-row selected in Figure 3(b) would constitute a particular reduced set.

It will be shown later that from a full set of GPSFs (N^{N_L}) only $N_L(N-1)+1$ are linearly independent. Evidently, it is as a result of this independence that a set of linearly independent GPSFs is not unique.

What remains now is to show that among N^{N_L} GPSFs extractable from a graph of NN_L local functional components $N_L(N-1)+1$ are effectively linearly independent. Their proper selection will follow as a result.

3.1.1. *Independence of GPSFs*

Figure 6 provides the basis of the following discussion. Figure 6 constitutes a sub-graph located on the top-left of a generic graph. This condition has been adopted only in order to simplify the nomenclature but it does not introduce any limit in the conclusions.

First of all, with respect to Figure 6, it should be noted that the functions (f_1, f_2, f_3) constitute three independent functions. The independence of the first two (f_1, f_2) is a merit of the respective polynomials that have an increasing degree (row by row, from the top to the bottom) and are evidently independent functions. The GPSF f_3 can be shown to be independent by a discussion *ab absurdo*: if we suppose that f_3 is a linear combination of (f_1, f_2) it means that f_{23} is also a locally linear combination of (f_{13}, f_{23}) (Figure 6). However, due to the correspondences in f_{23}, such local dependence can only be established by admitting that the coefficient of f_{13} is zero. Such a conclusion leads to the admission that f_3 is coincident with f_2. Figure 6 shows that this coincidence is not evidently true. An analogue discussion *ab absurdo* can be carried out to show that the set of GPSFs represented with continuous lines in Figure 7 $(f_1–f_6)$ are linearly independent.

Moreover, referring to Figure 7, it can be proved that any path can be obtained by a linear combination of the set $(f_1–f_6)$. First of all this can be proved by showing that f_4 (dashed line in Figure 6) can be expressed by a linear combination of (f_1, f_2, f_3). In this respect, functions around ξ_2 in Figure 6 $(f_{12}, f_{22}, f_{13}, f_{23})$ deserve attention in the following discussion.

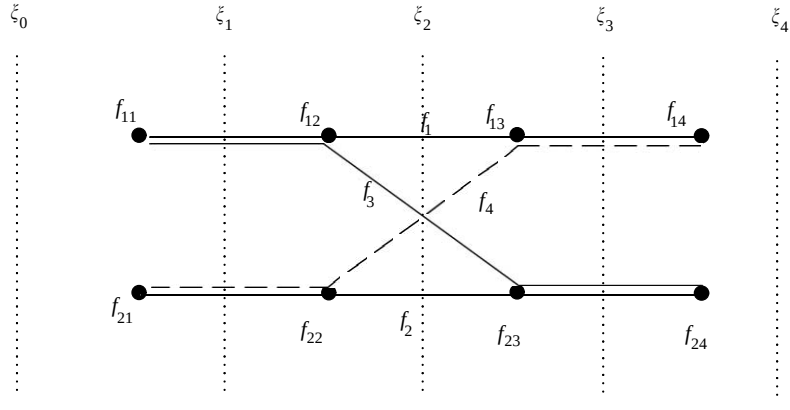

Figure 6. A basic set of linearly dependent GPSFs.

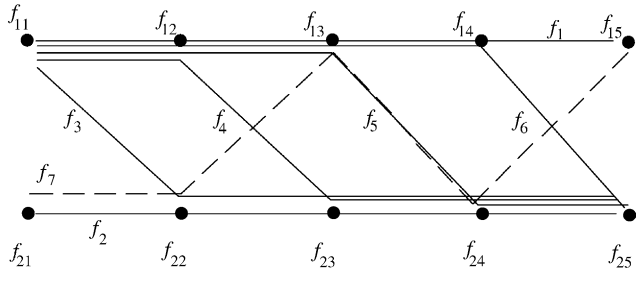

Figure 7. A basic set (—) of linearly independent GPSFs.

After considering the meaning of the scaling coefficients previously introduced in equation (27) and Figure 4, the following equation can be established:

$$C_{22,13}C_{12,23} = C_{12,13}C_{22,23}. \tag{29}$$

From equation (29) and still with respect to the functions around ξ_2, the following linear dependence (30) can be verified:

$$\begin{Bmatrix} f_{22} \\ C_{22,13}f_{13} \end{Bmatrix} = \bar{a}_1 \begin{Bmatrix} f_{12} \\ C_{12,13}f_{13} \end{Bmatrix} + \bar{a}_2 \begin{Bmatrix} f_{22} \\ C_{22,23}f_{23} \end{Bmatrix} + \bar{a}_3 \begin{Bmatrix} f_{12} & \xi \in (\xi_1, \xi_2) \\ C_{12,23}f_{23} & \xi \in (\xi_2, \xi_3) \end{Bmatrix} \tag{30}$$

whenever the global coefficients of linear combination $(\bar{a}_1, \bar{a}_2, \bar{a}_3)$ assume the following values:

$$(\bar{a}_1, \bar{a}_2, \bar{a}_3) = (C_{22,23}/C_{12,23},\ 1,\ -\bar{a}_1). \tag{31}$$

Moreover, if it is supposed that pairs of branches go into ξ_1 and go out of ξ_3 (Figure 6) then the relative arrangement of coefficients (31) is still able to preserve a global linear combination in the range $[\xi_0, \xi_4]$ whenever the first global coefficient $(\bar{a}_1)$ is recursively pre-multiplied by the coefficients preceding ξ_1. Namely, the following linear dependence (32):

$$\begin{Bmatrix} f_{21} \\ C_{21,22}f_{22} \\ C_{22,13}\ C_{21,22}f_{13} \\ C_{13,14}\ C_{22,13}\ C_{21,22}f_{14} \end{Bmatrix} = a_1 \begin{Bmatrix} f_{11} \\ C_{11,12}f_{12} \\ C_{12,13}\ C_{11,12}f_{13} \\ C_{13,14}\ C_{12,13}\ C_{11,22}f_{14} \end{Bmatrix} + a_2 \begin{Bmatrix} f_{21} \\ C_{21,22}f_{22} \\ C_{22,23}\ C_{21,22}f_{23} \\ C_{23,24}\ C_{22,23}\ C_{21,22}f_{24} \end{Bmatrix}$$

$$+ a_3 \begin{Bmatrix} f_{11}, & \xi \in (\xi_0,\ \xi_1), \\ C_{11,12}f_{12}, & \xi \in (\xi_1,\ \xi_2), \\ C_{12,23}\ C_{11,12}f_{23}, & \xi \in (\xi_2,\ \xi_3), \\ C_{23,24}\ C_{12,23}\ C_{11,12}f_{24}, & \xi \in (\xi_3,\ \xi_4), \end{Bmatrix} \tag{32}$$

can easily be verified once the following global coefficients (33) are taken into account together with condition (29):

$$(a_1, a_2, a_3) = \left(\frac{C_{21,22}}{C_{11,12}}\ \bar{a}_1,\ 1,\ -a_1 \right). \tag{33}$$

Equation (32) concludes the proof concerning the linear dependence of f_4 with respect to (f_1, f_2, f_3). However the proof was based on Figure 6 where the GPSFs are assumed to have pairs of branches going into and going out of the quadrant $(f_{12}, f_{22}, f_{13}, f_{23})$. The lack of this assumption for certain possible paths could limit the validity of the previous proof. For example, the dashed path (f_7) of Figure 7 could be a possible candidate for being an additional independent GPSF with respect to the aforesaid list $(f_1$–$f_6)$. However, it can be shown that the configuration corresponding to Figure 6 is always reproducible so that any path extraneous to the continuous lines of Figure 7 $(f_1$–$f_6)$, as for example f_7, is a linear

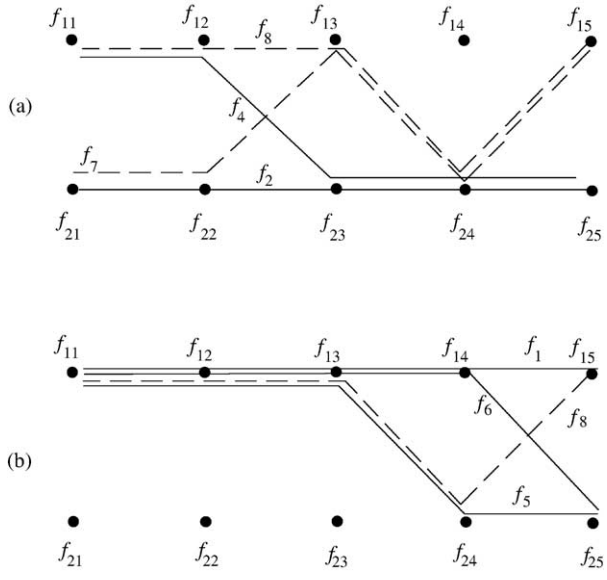

Figure 8. Reproduction of a set of linearly dependent GPSFs.

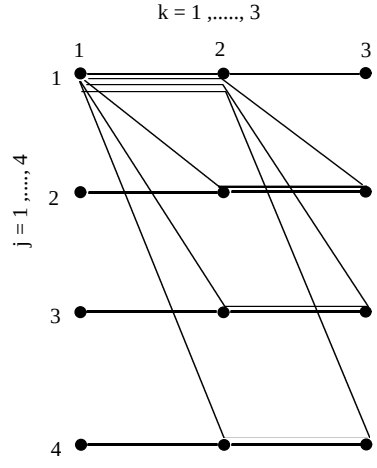

Figure 9. Selection of $N_L(N-1)+1$ linearly independent GPSFs at an expansion-level $N=4$ in $N_L=3$ sub-domains.

combination of (f_1–f_6). This can be seen in Figure 8 which reports one part of the paths shown in Figure 7. In particular, Figure 8(a) introduces a path (f_8) that after going out of f_{13} follows f_7 to terminate in f_{15}. In this way, a configuration similar to Figure 6 has been reproduced for the set (f_2, f_4, f_7, f_8) and, therefore, f_7 becomes a linear combination of (f_2, f_4, f_8). On the other hand, Figure 8(b) reproduces a configuration similar to Figure 6 for the set (f_1, f_5, f_6, f_8) and for this f_8 is a linear combination of (f_1, f_5, f_6). Therefore, f_7 is a linear combination of the functions (f_1, f_2, f_4, f_5, f_6). These latter belong to the basic set of independent GPSFs (f_1–f_6). In conclusion it can be stated that (f_1–f_6) represent a basic set of independent global piecewise-smooth functions of Figure 7.

An extrapolation of the aforesaid discussion is able to show that Figure 9 corresponds to a suitable set of $N_L(N-1)+1$ linearly independent GPSFs.

Therefore, once N has been fixed at a certain expansion level in a global domain constituted by N_L sub-domains, a suitable base of GPSFs is intended as a set of $N_L(N-1)+1$ functions properly selected from a graph. A proper selection should be intended as assembling a set of linearly independent approximating functions.

Some additional remarks are finally worth noting. The number of independent functions is not only dependent on the number of the components in each domain (N) but it linearly depends also on the number of sub-domains (N_L) containing the smooth pieces of a prescribed function $f(\xi)$. Therefore, an increasing presence of discontinuities (sub-domains) makes an approximation process automatically more demanding because it requires, at a local fixed degree of approximation (N), an increasing number of GPSFs.

The local independent functions used here in equation (26) constitute a possibility that is not believed to be unique. Indeed, the previous discussion dealt with the introduction of an algorithmic choice of algebraically manipulated known functions, rather than with the introduction of new and unique approximating functions.

3.1.2. *GPSFs: numerical tests*

In this section some numerical examples are reported in order to show the effectiveness of the aforesaid GPSFs. The numerical examples show how a global linear combination of convenient piecewise-smooth functions (illustrated in Figure 9) is able to realize a *best approximation in the mean* (equations (23) and (24)) to prescribed functions having different types of discontinuities. Four different kinds of functions were selected in order to test the performances of the GPSFs in a *best approximation in the mean* ((23), (24)). In all cases three different domains were considered to contain the smooth parts of the prescribed functions defined in $[-1/2,\ 1/2]$ and fulfilling the boundary conditions given in equation (25).

The approximating process in all cases is carried out by using the set of GPSFs illustrated in Figure 10. They correspond to a suitable selection of GPSFs (Figure 9) of SF, FF and FS bases up to $N = 3$ (26) for a total of seven functional components ($N_L(N-1)+1$).

Figure 11(a–d) illustrates the four numerical simulations. They show the related graphics of prescribed functions $f(\xi)$ shifted by a constant for a better visual inspection, their *best approximation in the mean* $f(\xi)_a$ and the difference $f(\xi)_a - f(\xi)$ shifted by value 1.

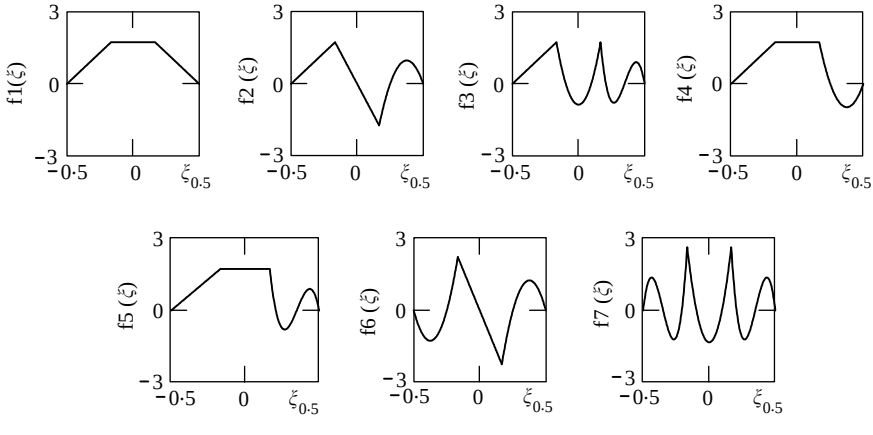

Figure 10. A polynomial set of $N_L(N-1)+1$ linearly independent GPSFs at an expansion-level $N = 3$ in $N_L = 3$ sub-domains.

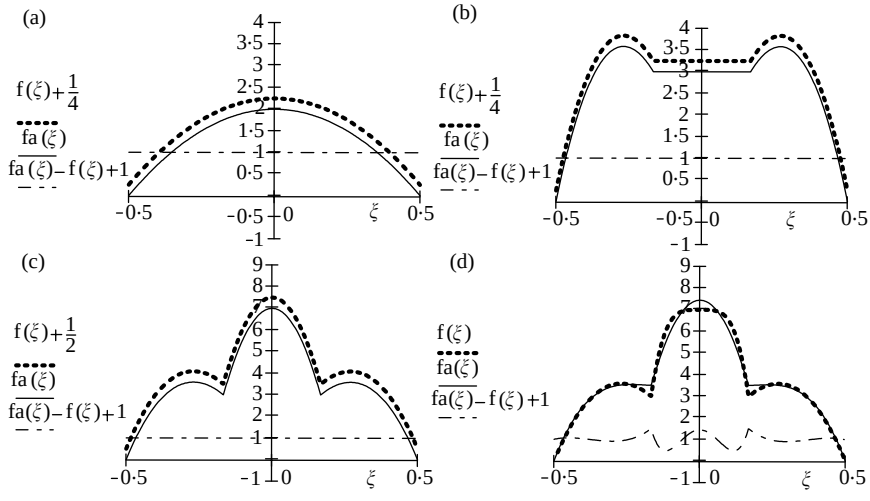

Figure 11. The *best approximation in the mean* to selected continuous functions by using GPSFs.

Figure 11(a) approximates to the mean the function.

$$f(\xi) = -8\xi^2 + 2, \qquad \xi \in (-1/2, 1/2). \tag{34}$$

This first case was chosen to test if the GPSFs (Figure 10) were naturally able to perform a suitable *best approximation in the mean* also for smooth continuous functions. This could be expected since a smooth continuous function should be seen as a particular case of a related function that presents certain discontinuities. Therefore, function (34) should be naturally accounted for by a generalized concept (GPSFs). The exact correspondence ($f(\xi)_a - f(\xi) = 0$ for any ξ in its range) can be explained by the degree of $f(\xi)$ (34) with respect to the degree of the approximating polynomials (26).

Figure 11(b, c) displays functions (35) and (36), respectively,

$$f(\xi) = \begin{cases} f(\xi)_1 = 36\xi^3 - 30\xi^2 - 24\xi, & \xi \in (-1/2, -1/6), \\ f(\xi)_2 = f(-1/6)_1, & \xi \in (-1/6, +1/6), \\ f(\xi)_3 = -36\xi^3 - 30\xi^2 + 24\xi, & \xi \in (+1/6, +1/2), \end{cases} \tag{35}$$

$$f(\xi) = \begin{cases} f(\xi)_1 = 36\xi^3 - 30\xi^2 - 24\xi, & \xi \in (-1/2, -1/6), \\ f(\xi)_2 = (f(-1/6)_1 - 7)\,36\xi^2 + 7, & \xi \in (-1/6, +1/6), \\ f(\xi)_3 = -36\xi^3 - 30\xi^2 + 24\xi, & \xi \in (+1/6, +1/2), \end{cases} \tag{36}$$

from which the best approximation in the mean by using the GPSFs of Figure 10 still provides an exact representation ($f(\xi)_a - f(\xi) = 0$ for any ξ in its range) of functions (35) and (36). Such exactness can still be explained through the polynomial degrees of the used GPSFs (26) with respect to the maximum local degrees in equations (35, 36).

Finally, Figure 11(d) shows the case corresponding to the equation

$$f(\xi) = \begin{cases} f(\xi)_1 = 36\xi^3 - 30\xi^2 - 24\xi, & \xi \in (-1/2, -1/6), \\ f(\xi)_2 = (f(-1/6)_1 - 7)\,6^4\xi^4 + 7, & \xi \in (-1/6, +1/6), \\ f(\xi)_3 = -36\xi^3 - 30\xi^2 + 24\xi, & \xi \in (+1/6, +1/2), \end{cases} \tag{37}$$

In this case the degree of the central polynomial in equation (37) is higher than the maximum degree considered in the relevant central domain of GPSFs-set ((26), Figure 10). Therefore, the set of GPSFs at a fixed $N = 3$ is unable to perform an exact representation of the prescribed function (37) by using equations (23, 24). A widespread error in $[-1/2, 1/2]$ is evident in Figure 11(d). This error is evidently caused by the global nature of the approximating process (23, 24).

The examples illustrated have shown the elegant performance of a set of GPSFs. Such set once realized *a priori* by simply scaling, delaying and turning over known functions (26), gives the possibility of approximating a C^0-continuous function independently by imposing explicitly internal continuity conditions. This characteristic would suggest the use, *a posteriori*, of a set of GPSFs in the present generalized mixed laminated plate theory.

4. FREELY VIBRATING CROSS-PLY SIMPLY SUPPORTED PLATES: NUMERICAL RESULTS

In this section the variational analytical model obtained in section 2 is tested in conjunction with the GPSFs presented in section 3. The numerical tests are performed to test the convergence of the present analytical model against functions that are in substance unknown because they are part of the relevant boundary value problem. The boundary value problem described by equations (20–22) cannot be solved by using closed-form solutions for any boundary condition, geometry and arrangement of layers involved. To this end, approximated numerical methods could be used. However, before solving the obtained boundary value problem by numerical methods, a test concerning its analytical performance remains to be of primary importance. Therefore, certain freely vibrating cross-ply plates which have been subjected to a certain class of simply supported constraints have been adopted because their exact solutions can be extracted from the present model and can be compared with existing exact results of the three-dimensional theory [24].

In particular, Nosier *et al.* [24], besides comparing different two-dimensional theories, published an extensive list of exact results in the frame of the three-dimensional theory. These results deal with rectangular laminated plates that according to Figure 1 are subjected to the following boundary conditions:

$$x = 0,\ L_x\colon\ v = w = 0;\ \sigma_x = 0, \quad z \in [-h/2,\ h/2],$$

$$y = 0,\ L_y\colon\ u = w = 0;\ \sigma_y = 0, \quad z \in [-h/2,\ h/2]. \tag{38}$$

As far as the present two-dimensional plate model is concerned, the simply supported edge boundary conditions that correspond to three-dimensional boundary conditions (38) are as follows:

$$x = 0,\ L_x\colon\ v_i = w_i = 0,\ N_{xi} = 0,$$

$$y = 0,\ L_y\colon\ u_i = w_i = 0,\ N_{yi} = 0 \tag{39}$$

and in this context the following displacement field:

$$u(x, y; t)_i = A^{ui} \cos \frac{m \cdot \pi \cdot x}{L_x} \sin \frac{n \cdot \pi \cdot y}{L_y} \cos(\omega_{mn} t),$$

$$v(x, y; t)_i = A^{vi} \sin \frac{m \cdot \pi \cdot x}{L_x} \cos \frac{n \cdot \pi \cdot y}{L_y} \cos(\omega_{mn} t),$$

$$w(x, y; t)_i = A^{wi} \sin \frac{m \cdot \pi \cdot x}{L_x} \sin \frac{n \cdot \pi \cdot y}{L_y} \cos(\omega_{mn} t) \tag{40}$$

fulfils exactly the boundary conditions of equations (39). Hence, once the Navier-type form of equations (20) have been specialized in accordance with equations (40) the following generalized eigenvalue problem (41) can be solved to evaluate the relevant exact frequencies (ω_{mn}):

$$(\mathbf{K} - \omega_{mn}^2 \mathbf{M})\,\mathbf{X} = \mathbf{0}, \tag{41}$$

where $\mathbf{X} = (A^{u1}, \ldots, A^{uN}, A^{v1}, \ldots, A^{vN}, A^{w1}, \ldots, A^{wN})^{\mathrm{T}}$ and stiffness and mass matrix assume for cross-ply arrangements the following expressions:

$$\mathbf{K} = \begin{bmatrix} p^2\bar{\mathbf{C}}_{11} + q^2\bar{\mathbf{C}}_{33} + \bar{\mathbf{C}}_{77} & pq[\bar{\mathbf{C}}_{12} + \bar{\mathbf{C}}_{34}] & p[\bar{\mathbf{C}}_{75} - \bar{\mathbf{C}}_{19}] \\ & q^2\bar{\mathbf{C}}_{22} + p^2\bar{\mathbf{C}}_{44} + \bar{\mathbf{C}}_{88} & q[\bar{\mathbf{C}}_{86} - \bar{\mathbf{C}}_{29}] \\ sym & & p^2\bar{\mathbf{C}}_{55} + q^2\bar{\mathbf{C}}_{66} + \bar{\mathbf{C}}_{99} \end{bmatrix}, \tag{42}$$

$$\mathbf{M} = \begin{bmatrix} \boldsymbol{\rho}_0^1 & 0 & 0 \\ & \boldsymbol{\rho}_0^2 & 0 \\ sym & & \boldsymbol{\rho}_0^3 \end{bmatrix} \quad \text{with} \quad \boldsymbol{\rho}_0^{\ell} = \begin{bmatrix} \rho_0^{\ell 1, \ell 1} & \cdots & \rho_0^{\ell 1, \ell N} \\ & \ddots & \vdots \\ sym & & \rho_0^{\ell N, \ell N} \end{bmatrix} \text{ and } \ell = 1, 2, 3 \tag{43}$$

having indicated with (p, q) quantities ($m\pi/L_x$) and ($n\pi/L_y$) respectively.

The performances of the present model (M3D) can be tested once a suitable base expanding the kinetic and stress quantities through the thickness of laminate (1, 2) is chosen *a posteriori* and introduced into the governing equation of motion (20–22).

The functions $(\alpha(z)_p, \beta(z)_p, \eta(z)_p)$ defined through the z-co-ordinate (i.e., $-1/2 \leqslant z/h = \xi \leqslant 1/2$) should be able to model globally the transverse stresses by equations (2), and also simultaneously to satisfy the boundary conditions on the top and the bottom of the plate ($\tau_{yz} = \tau_{xz} = \sigma_z = 0$). They have been chosen as GPSFs generated by equations (26), adapted in the relative sub-domains and assembled by using the scheme of Figure 9. These orthogonal polynomials, have been extensively used in vibration studies using the Ritz method (see, for example, references [21, 34–38]) and can be generated by known recursive equations [35].

The functions $(\Phi(z)_{1j}, \Phi(z)_{2j}, \Phi(z)_{3j})$ defined through the z-co-ordinate (i.e., $-1/2 \leqslant z/h = \xi \leqslant 1/2$) should be able to model globally the displacement components by equations (1). In the case of the displacement components, no boundary condition, apart from the inherent layer-by-layer continuity, needs to be satisfied. For this reason, all the local functional components were chosen to be coincident with FF-bases (equations (26)) adapted in the relevant sub-domains.

Therefore, once a GPSFs-base is fixed at an N expansion level for a laminated plate made of N_L layers, the eigenvalue problem (42) consists of matrices having order $3(N_L(N-1)+1) \times 3(N_L(N-1)+1)$. Under these considerations and with the usual convention that indicates through (1, 2, 3) the fibre direction, the transverse in-plane direction and the normal z direction, respectively, the following numerical tests concerning

TABLE 1

First 10 *frequency parameters,* $\hat{\omega}$*, for cross-ply square plates*; $[0^\circ/90^\circ/0^\circ/90^\circ]$; $Lx/h = 10$

		M3D; N, e%						LW4 [32]
	Exact [24]	3	e%	4	e%	5	6	
(1, 1)	0·06621	0·06621	0·00	0·06621	0·00	0·06621	0·06621	0·06621
	0·54596	0·54596	0·00	0·54596	0·00	0·54596	0·54596	0·54596
	0·59996	0·59996	0·00	0·59996	0·00	0·59996	0·59996	0·59996
	1·2425	1·2428	0·02	1·2425	0·00	1·2425	1·2425	1·2425
	1·2988	1·2992	0·03	1·2988	0·00	1·2988	1·2988	1·2987
	1·3265	1·3270	0·04	1·3265	0·00	1·3265	1·3265	1·3265
	2·3631	2·3653	0·09	2·3630	0·00	2·3631	2·3631	2·3631
	2·3789	2·3811	0·09	2·3789	0·00	2·3789	2·3789	2·3789
	2·4911	2·4938	0·11	2·4911	0·00	2·4911	2·4911	2·4911
	3·6661	3·6732	0·19	3·6695	0·09	3·6661	3·6661	2·6662
(2, 1)	0·15194	0·15195	0·01	0·15194	0·00	0·15194	0·15194	0·15194
	0·63875	0·63875	0·00	0·63875	0·00	0·63875	0·63875	0·63875
	1·0761	1·0762	0·01	1·0761	0·00	1·0761	1·0761	1·0761
	1·2417	1·2420	0·02	1·2417	0·00	1·2417	1·2417	1·2417
	1·3425	1·3429	0·03	1·3425	0·00	1·3425	1·3425	1·3425
	1·6323	1·6329	0·04	1·6323	0·00	1·6323	1·6323	1·6323
	2·3869	2·3892	0·10	2·3869	0·00	2·3869	2·3869	2·3869
	2·4844	2·4871	0·11	2·4844	0·00	2·4844	2·4844	2·4844
	2·5614	2·5640	0·10	2·5614	0·00	2·5614	2·5614	2·5614
	3·6778	3·6861	0·23	3·6808	0·08	3·6778	3·6778	3·6778

Tables 1–3 were performed on the assumption that the laminated plates investigated are characterized by the following material properties:

$$E_1 = 25{\cdot}1 \times 10^6 \text{ psi}, \; E_2 = 4{\cdot}8 \times 10^6 \text{ psi}, \; E_3 = 0{\cdot}75 \times 10^6 \text{ psi},$$

$$G_{12} = 1{\cdot}36 \times 10^6 \text{ psi}, \; G_{13} = 1{\cdot}2 \times 10^6 \text{ psi}, \; G_{23} = 0{\cdot}47 \times 10^6 \text{ psi},$$

$$v_{12} = 0{\cdot}036, \; v_{13} = 0{\cdot}25, \; v_{23} = 0{\cdot}171, \tag{44}$$

by listing a dimensionless frequency parameter such as in equation (45):

$$\hat{\omega} = \omega h \sqrt{\rho / E_2}. \tag{45}$$

As far as the numerical tests of Table 4 are concerned, different material properties were used. They correspond to laminated plates made of transversely isotropic materials with constants as reported in

$$E_1 = 40E_2 = 40E_3, \quad G_{12} = G_{13} = 0{\cdot}6E_2, \quad G_{23} = 0{\cdot}5E_2, \quad v_{12} = v_{13} = 0{\cdot}25. \tag{46}$$

The relevant dimensionless frequency parameter of Table 4 corresponds to the following expression:

$$\bar{\omega} = \omega \frac{L_x^2}{h} \sqrt{\rho / E_2}. \tag{47}$$

TABLE 2

First 10 *frequency parameters,* $\hat{\omega}$*, for cross-ply square plates*; $[0^\circ/90^\circ/0^\circ]$; $Lx/h = 10$

		M3D; N, e%							
(m, n)	Exact [24]	3	e%	4	e%	5	e%	6	7
(1, 1)	0·06715	0·06715	0·00	0·06715	0·00	0·06715	0·00	0·06715	0·06715
	0·50350	0·50349	0·00	0·50349	0·00	0·50349	0·00	0·50349	0·50349
	0·63775	0·63775	0·00	0·63775	0·00	0·63775	0·00	0·63775	0·63775
	1·2429	1·2437	0·06	1·2429	0·00	1·2429	0·00	1·2429	1·2429
	1·2790	1·2800	0·08	1·2790	0·00	1·2790	0·00	1·2790	1·2790
	1·3292	1·3308	0·12	1·3292	0·00	1·3292	0·00	1·3292	1·3292
	2·1533	2·1565	0·15	2·1535	0·01	2·1533	0·00	2·1533	2·1533
	2·4894	2·4968	0·30	2·4900	0·02	2·4894	0·00	2·4894	2·4894
	2·7419	2·7533	0·42	2·7471	0·19	2·7419	0·00	2·7419	2·7419
	3·5416	3·6233	2·31	3·5401	− 0·04	3·5424	0·02	3·5416	3·5416
(2, 1)	0·17217	0·17220	0·02	0·17217	0·00	0·17217	0·00	0·17217	0·17217
	0·58366	0·58366	0·00	0·58366	0·00	0·58366	0·00	0·58366	0·58366
	1·1780	1·1783	0·03	1·1780	0·00	1·1780	0·00	1·1780	1·1780
	1·2752	1·2758	0·05	1·2752	0·00	1·2752	0·00	1·2752	1·2752
	1·3141	1·3151	0·08	1·3141	0·00	1·3141	0·00	1·3141	1·3141
	1·7778	1·7815	0·21	1·7778	0·00	1·7778	0·00	1·7778	1·7778
	2·1724	2·1755	0·14	2·1725	0·00	2·1724	0·00	2·1724	2·1724
	2·4925	2·5000	0·30	2·4931	0·02	2·4925	0·00	2·4925	2·4925
	2·8899	2·9011	0·39	2·8958	0·20	2·8899	0·00	2·8899	2·8899
	3·5533	3·6347	2·29	3·5518	− 0·04	3·5540	0·02	3·5533	3·5533

Tables 1–3 report a convergence test for the present generalized two-dimensional laminated plate model when an increasing number of GPSFs is used. All these tables report the first 10 frequency parameters for fixed wave numbers listed in brackets in the first column for each table. The columns corresponding to the present theory (M3D) represent the frequency parameters until the expansion level of GPSFs obtained a convergence for the first five significant digits. Moreover, to the right-hand side of the columns of frequencies, columns of percentage errors, calculated using both the results of the present model and the exact three-dimensional results published in reference [24], are reported.

Tables 1–3 clearly show how the performances of the present model are excellent and stable. Indeed, the present model never failed to get the exact results. Moreover, the convergence process is shown to be extremely fast. An expansion level $N = 4$ is indeed able to get an accuracy in the frequencies that meet many engineering applications. In any case, the present model seems to offer the choice of increasing the expansion level (N) until a sufficient convergence is achieved. In this respect, a perusal of Tables 1–3 shows that, in particular, it is clear that the convergence process undergoes, though it is not really serious, a certain dependence on the layout of the layers through the thickness. Indeed, the best performance of the model was obtained in the case of Table 1 where four layers constituted the laminate. In this case the full convergence was obtained with $N = 5$. Conversely, the worst case was obtained for Table 3 where two layers, in an antisymmetric configuration, constituted the laminate. In this case the full convergence was obtained with $N = 7$. All the relevant exact results reported in reference [24, Table 2] were obtained exactly by the present theory (here reported only in part in Tables 1–3 for the sake of brevity) with performances similar to Tables 1–3. Therefore, the numerical comparisons stress the importance to have a model available, depending on the particular case studied, which

TABLE 3

First 10 *frequency parameters,* $\hat{\omega}$*, for cross-ply square plates*; [0°/90°]; $Lx/h = 10$

		M3D; N, e%								
(m, n)	Exact [24]	3	e%	4	e%	5	e%	6	e%	7
(1, 1)	0·06027	0·06031	0·07	0·06027	0·00	0·06027	0·00	0·06027	0·00	0·06027
	0·52994	0·52994	0·00	0·52994	0·00	0·52994	0·00	0·52994	0·00	0·52994
	0·58275	0·58276	0·00	0·58275	0·00	0·58275	0·00	0·58275	0·00	0·58275
	1·2367	1·2405	0·31	1·2368	0·01	1·2367	0·00	1·2367	0·00	1·2367
	1·2793	1·2840	0·37	1·2794	0·01	1·2793	0·00	1·2793	0·00	1·2793
	1·2977	1·3029	0·40	1·2978	0·01	1·2977	0·00	1·2977	0·00	1·2977
	2·4730	2·4956	0·91	2·4751	0·08	2·4731	0·00	2·4730	0·00	2·4730
	2·5658	2·6222	2·20	2·5728	0·27	2·5664	0·02	2·5658	0·00	2·5658
	2·5736	2·6230	1·92	2·5782	0·18	2·5741	0·02	2·5736	0·00	2·5736
	3·5811	3·6566	2·11	3·7038	3·43	3·5820	0·03	3·5825	0·04	3·5811
(2, 1)	0·14539	0·14557	0·12	0·14539	0·00	0·14539	0·00	0·14539	0·00	0·14539
	0·62352	0·62353	0·00	0·62352	0·00	0·62352	0·00	0·62352	0·00	0·62352
	0·95652	0·95659	0·01	0·95652	0·00	0·95652	0·00	0·95652	0·00	0·95652
	1·2389	1·2424	0·28	1·2390	0·01	1·2389	0·00	1·2389	0·00	1·2389
	1·3189	1·3238	0·37	1·3189	0·00	1·3189	0·00	1·3189	0·00	1·3189
	1·6583	1·6668	0·51	1·6584	0·01	1·6584	0·01	1·6583	0·00	1·6583
	2·4676	2·4899	0·90	2·4700	0·10	2·4677	0·00	2·4676	0·00	2·4676
	2·5843	2·6378	2·07	2·5905	0·24	2·5849	0·02	2·5843	0·00	2·5843
	2·7110	2·7702	2·18	2·7192	0·30	2·7118	0·03	2·7110	0·00	2·7110
	3·5966	3·6726	2·11	3·7177	3·37	3·5977	0·03	3·5980	0·04	3·5966

TABLE 4

Fundamental frequency parameters, $\bar{\omega}$*, of* [0°/90°] *laminated square plates against length/thickness ratio*

		M3D			LWPT [24]		
Lx/h	Exact [24]	$N = 3$ 15†	$N = 5$ 27†	$N = 7$ 39†	$N = 12$ 39‡	$N = 20$ 63‡	$N = 30$ 93‡
2	4·935	4·948	4·936	4·935	4·957	4·944	4·939
5	8·518	8·560	8·518	8·518	4·541	8·526	8·521
10	10·333	10·356	10·333	10·333	10·344	10·337	10·335
20	11·036	11·043	11·036	11·036	11·039	11·037	10·036
25	11·131	11·136	11·131	11·131	11·134	11·132	11·132
50	11·263	11·265	11·263	11·263	11·264	11·264	11·263
100	11·297	11·298	11·297	11·297	11·298	11·297	11·297

† $6(N - 1) + 3$.
‡ $3(N + 1)$.

may be able to improve the accuracy of the results by simply changing a controllable parameter (N).

Finally, the comparison of the present model (M3D) with respect to the results obtained by LW4 [32] in Table 1 is interesting. Apart from a possible printing error (2·6662) and a slight discrepancy (1·2987), the performances concerning LW4 seem to be equivalent for

the particular case of the M3D-model corresponding to a fixed expansion level of $N = 5$. This should not come as a surprise because in reference [32] suitable Legendre polynomials were used up to a comparable expansion level of $N = 5$. Unfortunately, reference [32] did not apply LW4 beyond four layers and a full comparison (suggested by Tables 1–3) with the present theory could not be performed. Therefore, the interesting equivalencies between the present model and the layerwise model presented in reference [32] should be confined to the comparisons analyzed in Table 1. In particular, the correspondences of Table 1 confirm what was to be expected by using the GPSFs: without burdening the computational effort the dynamics of freely vibrating multilayered plates can also be considered by modelling the relevant kinetic and stress quantities in a global sense (by GPSFs) as well as in a local sense (i.e., expanding quantities for each layer). Such a choice permits the global differential equations of motion to be defined directly on the middle plane of the whole laminate (π_{xy} of Figure 1) through $3(N_L N + 1 - N_L)$ displacement degrees of freedom. The *a posteriori* choice of GPSFs makes the present theory automatically able to satisfy interlaminar continuities and external boundary conditions. These characteristics give the present model similar characteristics to the well-known two-dimensional global models (CPT, FSDT, HSDT) with the further ability to approach the exact three-dimensional results. Conversely, LW4 [31, 32] consists of a layerwise theory whose displacement degrees of freedom are strictly dependent on layer-by-layer quantities. Model LW4 is therefore, implicitly related to the complexity of the multilayered plate. The more refined formulation of the present model, obtained here as an extension of reference [22], should therefore make the model more preferable.

Finally, Table 4 reports some numerical comparisons between the present model (M3D) and a displacement-based layerwise theory (LWPT) [24]. In this respect, two possible printing errors (4·541, 10·036) should be excluded from the comparisons. Table 4 reports frequency parameter (48) with respect to square plates having various length/thickness ratios, from very thick ($L_x/h = 2$) to quite thin plates ($L_x/h = 100$). In Table 4 again a convergence test for the present model (M3D) is carried out by increasing the expansion level N. It is stressed that, as far as Table 4 is concerned, the parameter N reported for both the compared models (M3D, LWPT) has a different meaning. However, in both models this parameter gives the number of unknowns involved in the corresponding equation of the motion once the number of layers has been established. This number of unknowns is assessed as shown at the bottom of Table 4 and it is assumed to be characteristic for the computational effort involved.

It can be seen that the present theory (M3D) shows once again an excellent performance. Indeed, it always gave the exact results. This performance is not greatly influenced by the length/thickness ratio. In particular, the convergence to the exact results is slightly slower with respect to the thickest plate ($L_x/h = 2$), for which $N = 7$ was required to get the full convergence at the first four significant digits. However, besides this exceptional case ($L_x/h = 2$), $N = 5$ was able to provide an excellent performance.

As far as the comparison of the present theory with LWPT [24] is concerned, it is evident that the M3D is computationally less time consuming. For example, the case corresponding to $N = 5$ in the M3D theory requires 27 degrees of freedom and lists frequencies whose accuracy is superior when compared with all cases obtained from the LWPT which, on the other hand, requires a higher number of degrees of freedom (39, 63, 93). Finally, it should be noted that the M3D always produced the exact results for the three-dimensional theory but the LWPT was able to similarly reach this accuracy only for the two thinnest plates ($L_x/h = 50, 100$) by using 93 degrees of freedom.

It is believed that the comparisons between the present theory and those few relevant theories existing in literature have not only shown the performance of a two-dimensional

model for vibrational studies of multilayered plates. It was further proved that a multilayered plate can be treated as if it were virtually made of a single layer. The mixed nature of the problem (i.e., continuum and discrete aspects coexisting in a multilayered plate) was considered in a unified manner by means of the GPSFs. In this latter respect, it is believed that this novel base (GPSFs) could be applied to other scientific applications where continuous and discrete aspects coexist.

Finally, Tables 1–3, should be helpful for testing the performances of future approximate two-dimensional theories as far as their convergence rate for a fixed computational effort (N) is concerned.

5. CONCLUSIONS

In this study, a previous study [22] that had already generalized two-dimensional higher order theories has been further extended to eliminate its inherent limitations. Namely, all the transverse stresses have been taken into account (shear and normal stresses) and both the transverse stresses and displacement components are modelled as C^0-continuous functions through the whole thickness of the laminated plate.

The present two-dimensional laminate plate theory has been derived by Reissner's mixed variational theorem [27]. It is based on the expansion of kinetic and stress quantities through the whole thickness of the multilayered plates by using arbitrary functions. It is suggested that such an arbitrariness should be controlled by complete bases where each single functional component satisfies the external boundary conditions for the transverse stresses and continuity conditions for both transverse stresses and displacement components.

In order to apply the present theory by using *a posteriori* arbitrary functions whilst simultaneously fulfilling boundary conditions and continuity requirements, a proper novel base has been developed. It is characterized by functions which have discontinuous derivatives (GPSFs) and are globally defined in the domain of interest (the whole thickness of the plate). Since it is believed the GPSFs might be helpful in other several applications apart from the present context they have been introduced in the frame of the *best approximation in the mean* to a prescribed function. Independence, uniqueness and numerical efficiency have also been discussed and tested.

The conjunction of the present two-dimensional laminated plate theory (M3D) with the novel global piecewise-smooth functions (GPSFs) has been shown to provide the exact results of the three-dimensional theory for several cases. Previous layerwise theories can be considered as particular cases of the present model or less accurate compared with the relevant computational effort.

The layerwise character of the present model naturally comes from the GPSFs used because the number of the functions required automatically increases with the number of layers involved. However, whenever a high number of layers is involved, a lower expansion level can be used to control the computational effort. It would be interesting to investigate whether an optimizing numerical process exists to further accelerate the convergence, by using a reduced number of functional components with respect to the layout involved and without excessively sacrificing the accuracy of the results.

ACKNOWLEDGMENTS

A mio padre.

REFERENCES

1. S. P. TIMOSHENKO 1921 *Philosophical Magazine* **41**, 744–746. On the correction for shear of the differential equation for transverse vibrations of prismatic bars.
2. E. REISSNER 1945 *Journal of Applied Mechanics* **12**, A69–A77. The effects of transverse shear deformation on the bending of elastic plates.
3. R. D. MINDLIN 1951 *Journal of Applied Mechanics* **18**, 31–38. Influence of rotatory inertia and shear on flexural motions of isotropic elastic plates.
4. A. W. LEISSA 1969 *Vibration of Plates*. NASA SP-160. Edition reprinted by Acoustical Society of America, Washington, 1993.
5. K. M. LIEW, C. M. WANG, Y. XIANG and S. KITIPORNCHAI 1998 *Vibration of Mindlin Plates*. Oxford: Elsevier.
6. K. H. LO, R. M. CHRISTENSEN and E. M. WU 1977 *Journal of Applied Mechanics* **44**, 663–668. A high-order theory of plate deformation. Part 1: homogeneous plates.
7. K. H. LO, R. M. CHRISTENSEN and E. M. WU 1977 *Journal of Applied Mechanics* **44**, 669–676. A high-order theory of plate deformation. Part 2: laminated plates.
8. A. BHIMARADDI and L. K. STEVENS 1984 *Journal of Applied Mechanics* **51**, 195–198. A high-order theory for free vibration of orthotropic, homogeneous, and laminated rectangular plates.
9. J. N. REDDY 1984 *Journal of Applied Mechanics* **51**, 745–752. A simple higher-order theory for laminated composite plates.
10. J. N. REDDY and N. D. PHAN 1985 *Journal of Sound and Vibration* **98**, 157–170. Stability and vibration of isotropic, orthotropic and laminated plates according to a higher order shear-deformation theory.
11. K. P. SOLDATOS 1988 *Journal of Applied Mechanics* **55**, 994–995. On certain refined theories for plate bending.
12. J. N. REDDY 1996 *Mechanics of Laminated Composite Plates, Theory and Analysis*. New York: CRC Press.
13. C. T. SUN and J. M. WHITNEY 1973 *American Institute of Aeronautics and Astronautics Journal* **11**, 178–183. Theories for the dynamic response of laminated plates.
14. P. C. CHOU and J. CARLEONE 1973 *American Institute of Aeronautics and Astronautics Journal* **11**, 1333–1336. Transverse shear in laminated plate theories.
15. M. DI SCIUVA 1986 *Journal of Sound and Vibration* **105**, 425–442. Bending, vibration and buckling of simply supported and thick multilayered orthotropic plates: an evaluation of a new displacement model.
16. M. DI SCIUVA 1992 *Composite Structures* **22**, 149–167. Multilayered anisotropic plate models with continuous interlaminar stresses.
17. K. P. SOLDATOS and T. TIMARCI 1993 *Composite Structures* **25**, 165–171. A unified formulation of laminated composite, shear deformable, five-degrees-of-freedom cylindrical shell theories.
18. T. TIMARCI and K. P. SOLDATOS 1995 *Journal of Sound and Vibration* **187**, 609–624. Comparative dynamic studies for symmetric cross-ply circular cylindrical shells on the basis of a unified shear deformable shell theory.
19. E. CARRERA 1997 *Composite Structures* **37**, 373–383. C_z^0 requirements-models for the two dimensional analysis of multilayered structures.
20. A. MESSINA and K. P. SOLDATOS 1999 *Journal of Acoustical Society of America* **106**, 2608–2620. Influence of edge boundary conditions on the free vibrations of cross-ply laminated circular cylindrical panels.
21. A. MESSINA and K. P. SOLDATOS 1999 *Journal of Sound and Vibration* **227**, 749–768. Ritz-type dynamic analysis of cross-ply laminated circular cylinders subjected to different boundary conditions.
22. A. MESSINA 2001 *Journal of Sound and Vibration* **242**, 125–150. Two generalized higher order theories in free vibration studies of multilayered plates.
23. J. N. REDDY 1987 *Communications in Applied Numerical Methods* **3**, 173–180. A generalization of two-dimensional theories of laminated composite plates.
24. A. NOSIER, R. K. KAPANIA and J. N. REDDY 1993 *American Institute of Aeronatics and Astronautics Journal* **31**, 2335–2346. Free vibration analysis of laminated plates using a layerwise theory.
25. K. P. SOLDATOS 1992 *Composite Structures* **20**, 195–211. A general plate theory accounting for continuity of displacements and transverse shear stresses at material interfaces.
26. E. REISSNER 1984 *International Journal for Numerical Methods in Engineering* **20**, 1366–1368. On a certain mixed variational theorem and a proposed application.
27. E. REISSNER 1986 *International Journal for Numerical Methods in Engineering* **23**, 193–198. On a mixed variational theorem and on shear deformable plate theory.

28. H. MURAKAMI 1986 *Journal of Applied Mechanics* **53**, 661–666. Laminated composite plate theory with improved in-plane responses.
29. A. TOLEDANO and H. MURAKAMI 1987 *Journal of Applied Mechanics* **54**, 181–188. A composite plate theory for arbitrary laminate configurations.
30. E. CARRERA 1998 *Journal of Applied Mechanics* **65**, 820–828. Layerwise mixed models for accurate vibrations analysis of multilayered plates.
31. E. CARRERA 1999 *Journal of Applied Mechanics* **66**, 69–78. A Reissner's mixed variational theorem applied to vibration analysis of multilayered shell.
32. E. CARRERA 1999 *Journal of Sound and Vibration* **225**, 803–829. A study of transverse normal stress effect on vibration of multilayered plates and shells.
33. G. SANSONE 1959 in *Orthogonal Functions* (R. Courant, L. Bers and J. J. Stoker, editors), Vol. IX, London: Interscience Publishers. (English edition translated from the Italian by A. Diamond and E. Hille.)
34. R. B. BATH 1985 *Journal of Sound and Vibration* **102**, 493–499. Natural frequencies of rectangular plates using characteristic orthogonal polynomials in Rayleigh–Ritz method.
35. T. S. CHIHARA 1978 *An Introduction to Orthogonal Polynomials*. New York: Gordon and Breach.
36. S. M. DICKINSON and A. DI BLASIO 1986 *Journal of Sound and Vibration* **108**, 51–62. On the use of orthogonal polynomials in the Rayleigh–Ritz method for the study of the flexural vibration and buckling of isotropic and orthotropic rectangular plates.
37. P. S. FREDERIKSEN 1995 *Journal of Sound and Vibration* **186**, 743–759. Single-layer plate theories applied to the flexural vibration of completely free thick laminates.
38. K. M. LIEW 1996 *Journal of Sound and Vibration* **198**, 343–360. Solving the vibration of thick symmetric laminates by Reissner/Mindlin plate theory and the P-Ritz method.
39. R. W. HAMMING 1962 *Numerical Methods for Scientists and Engineers*. New York: Dover Publications.
40. J. M. WHITNEY 1987 *Structural Analysis of Laminated Anisotropic Plates*. Lancaster: Technomic.

APPENDIX A: MATRICES IN EQUATION (22)

$$\bar{\mathbf{C}}_{11} = \int_{-h/2}^{h/2} Q_{11}^k \boldsymbol{\Phi}_1 \boldsymbol{\Phi}_1^{\mathrm{T}} \, \mathrm{d}z + \mathbf{B}_{32}^{u\mathrm{T}} \mathbf{G}_{33} \mathbf{B}_{32}^{u}, \qquad \bar{\mathbf{C}}_{12} = \int_{-h/2}^{h/2} Q_{12}^k \boldsymbol{\Phi}_1 \boldsymbol{\Phi}_2^{\mathrm{T}} \, \mathrm{d}z + \mathbf{B}_{32}^{u\mathrm{T}} \mathbf{G}_{33} \mathbf{B}_{33}^{v},$$

$$\bar{\mathbf{C}}_{13} = \int_{-h/2}^{h/2} Q_{16}^k \boldsymbol{\Phi}_1 \boldsymbol{\Phi}_1^{\mathrm{T}} \, \mathrm{d}z + \mathbf{B}_{32}^{u\mathrm{T}} \mathbf{G}_{33} \mathbf{B}_{32}^{u}, \qquad \bar{\mathbf{C}}_{14} = \int_{-h/2}^{h/2} Q_{16}^k \boldsymbol{\Phi}_1 \boldsymbol{\Phi}_2^{\mathrm{T}} \, \mathrm{d}z + \mathbf{B}_{32}^{u\mathrm{T}} \mathbf{G}_{33} \mathbf{B}_{32}^{v},$$

$$\bar{\mathbf{C}}_{22} = \int_{-h/2}^{h/2} Q_{22}^k \boldsymbol{\Phi}_2 \boldsymbol{\Phi}_2^{\mathrm{T}} \, \mathrm{d}z + \mathbf{B}_{33}^{v\mathrm{T}} \mathbf{G}_{33} \mathbf{B}_{33}^{v}, \qquad \bar{\mathbf{C}}_{23} = \int_{-h/2}^{h/2} Q_{26}^k \boldsymbol{\Phi}_2 \boldsymbol{\Phi}_1^{\mathrm{T}} \, \mathrm{d}z + \mathbf{B}_{33}^{v\mathrm{T}} \mathbf{G}_{33} \mathbf{B}_{33}^{u},$$

$$\bar{\mathbf{C}}_{24} = \int_{-h/2}^{h/2} Q_{26}^k \boldsymbol{\Phi}_2 \boldsymbol{\Phi}_2^{\mathrm{T}} \, \mathrm{d}z + \mathbf{B}_{33}^{v\mathrm{T}} \mathbf{G}_{33} \mathbf{B}_{32}^{v}, \qquad \bar{\mathbf{C}}_{33} = \int_{-h/2}^{h/2} Q_{66}^k \boldsymbol{\Phi}_1 \boldsymbol{\Phi}_1^{\mathrm{T}} \, \mathrm{d}z + \mathbf{B}_{33}^{u\mathrm{T}} \mathbf{G}_{33} \mathbf{B}_{32}^{v},$$

$$\bar{\mathbf{C}}_{34} = \int_{-h/2}^{h/2} Q_{66}^k \boldsymbol{\Phi}_1 \boldsymbol{\Phi}_2^{\mathrm{T}} \, \mathrm{d}z + \mathbf{B}_{33}^{u\mathrm{T}} \mathbf{G}_{33} \mathbf{B}_{32}^{v}, \qquad \bar{\mathbf{C}}_{44} = \int_{-h/2}^{h/2} Q_{66}^k \boldsymbol{\Phi}_2 \boldsymbol{\Phi}_2^{\mathrm{T}} \, \mathrm{d}z + \mathbf{B}_{32}^{v\mathrm{T}} \mathbf{G}_{33} \mathbf{B}_{32}^{v},$$

$$\bar{\mathbf{C}}_{19} = \mathbf{B}_{32}^{u\mathrm{T}} \mathbf{G}_{33} \mathbf{B}_{31}^{w}, \quad \bar{\mathbf{C}}_{29} = \mathbf{B}_{33}^{v\mathrm{T}} \mathbf{G}_{33} \mathbf{B}_{31}^{w}, \quad \bar{\mathbf{C}}_{39} = \mathbf{B}_{33}^{u\mathrm{T}} \mathbf{G}_{33} \mathbf{B}_{31}^{w}, \quad \bar{\mathbf{C}}_{49} = \mathbf{B}_{32}^{v\mathrm{T}} \mathbf{G}_{33} \mathbf{B}_{31}^{w},$$

$$\bar{\mathbf{C}}_{55} = \mathbf{B}_{22}^{w\mathrm{T}} \mathbf{G}_{22} \mathbf{B}_{22}^{w}, \quad \bar{\mathbf{C}}_{56} = \mathbf{B}_{22}^{w\mathrm{T}} \mathbf{G}_{12}^{\mathrm{T}} \mathbf{B}_{13}^{w}, \quad \bar{\mathbf{C}}_{57} = \mathbf{B}_{22}^{w\mathrm{T}} \mathbf{G}_{22} \mathbf{B}_{21}^{u}, \quad \bar{\mathbf{C}}_{58} = \mathbf{B}_{22}^{w\mathrm{T}} \mathbf{G}_{12}^{\mathrm{T}} \mathbf{B}_{11}^{v},$$

$$\bar{\mathbf{C}}_{66} = \mathbf{B}_{13}^{w\mathrm{T}} \mathbf{G}_{11} \mathbf{B}_{13}^{w}, \quad \bar{\mathbf{C}}_{67} = \mathbf{B}_{13}^{w\mathrm{T}} \mathbf{G}_{12} \mathbf{B}_{21}^{u}, \quad \bar{\mathbf{C}}_{68} = \mathbf{B}_{13}^{w\mathrm{T}} \mathbf{G}_{11} \mathbf{B}_{11}^{v}, \quad \bar{\mathbf{C}}_{77} = \mathbf{B}_{21}^{u\mathrm{T}} \mathbf{G}_{22} \mathbf{B}_{21}^{u},$$

$$\bar{\mathbf{C}}_{78} = \mathbf{B}_{21}^{u\mathrm{T}} \mathbf{G}_{12}^{\mathrm{T}} \mathbf{B}_{11}^{v}, \quad \bar{\mathbf{C}}_{88} = \mathbf{B}_{11}^{v\mathrm{T}} \mathbf{G}_{11} \mathbf{B}_{11}^{v}, \quad \bar{\mathbf{C}}_{99} = \mathbf{B}_{31}^{w\mathrm{T}} \mathbf{G}_{33} \mathbf{B}_{31}^{w}.$$

where Q_{ij}^k are the reduced stiffnesses [40] and $(\boldsymbol{\Phi}_1, \boldsymbol{\Phi}_2, \boldsymbol{\Phi}_3)$ are vectors assembled with ordered global approximating functions $(\boldsymbol{\Phi}(z)_{1j}, \boldsymbol{\Phi}(z)_{2j}, \boldsymbol{\Phi}(z)_{3j})$ respectively.